DEVELOPMENT OF A BORONIC ACID SENSOR-BASED GLUCOSE-RESPONSIVE NANOPARTICULATE INSULIN DELIVERY SYSTEM

NABIL AHMAD SIDDIQUI

MASTER OF PHARMACY

Thesis submitted to The University of Nottingham for the degree of

Master of Philosophy

September 2016

Abstract

Diabetes is one of the most common chronic diseases in the world and its incidence is on the rise. Maintenance of continuous normoglycaemic conditions is the key goal for the management of both type 1 and type 2 diabetes in patients. Glucose responsive insulin delivery (GRID) systems have the potential to act as artificial pancreas as they can modulate the insulin release relative to external glucose concentrations. GRIDs can not only achieve tighter glycaemic control by preventing both hypo- and hyperglycaemia, but also eliminate the need for frequent finger-stick glucose tests and multiple daily insulin injections. In this research, we examined the selectivity of and insulin release from two boronic acids (2-formyl-3-thienylboronic acid (FTBA) and 4-formylphenylboronic acid (FPBA)) to glucose when conjugated to chitosan as nanoparticles. Adsorption of glucose to BA: chitosan conjugates was dose-dependent up to 1:1 at 35 and 42% for FPBA and FTBA respectively but the FTBA conjugates adsorbed more glucose and fructose at respective FPBA ratios. The affinity of both BA conjugates to glucose decreased with increase in BA ratio. On the other hand, the affinity of both BA conjugates for fructose decreased from ratio 1:1 to 2:1 then rose again at 3:1. Insulin release from FPBA nanoparticles (FPBAINP) and FTBA nanoparticles (FTBAINP) were both concentration-dependent within glyceamically relevant values (1-3mg/ml glucose and 0.002mg/ml fructose). Furthermore, the total amounts of insulin released from FPBAINP in both the media were higher than from FTBAINP. Both FPBAINP and FTBAINP have the potential for development as a glucose-selective insulin delivery system in physiological settings.

Acknowledgements

I would like to express my utmost gratitude to Professor Nashiru Billa for choosing me as one of his postgraduate students and providing me with guidance throughout this exceptional research project. I also thank all the technicians for providing me with the necessary training in handling various instruments throughout my MPhil degree.

List of contents

Abbreviations

GRID	Glucose-responsive insulin delivery
BA	Boronic acid
FPBA	4-formylphenylboronic acid
FTBA	2-formyl-3-thienylboronic
FTIR	Fourier transform infrared spectroscopy
DSC	Differential scanning calorimetry
HPLC	High Performance Liquid Chromatography
NAD^+	Nicotinamide adenine dinucleotide (oxidised)
NADH	Nicotinamide adenine dinucleotide (reduced)
UV	Ultraviolet (spectroscopy)
CS	Chitosan
TPP	Tripolyphosphate
INP	Insulin Nanoparticle

CHAPTER 1

BACKGROUND AND OBJECTIVES

1.1. Overview of diabetes

Diabetes mellitus is a medical disorder involving high blood glucose levels – hyperglycaemia [1]. As one of the most common chronic diseases in almost every country in the world, the incidence of diabetes is on the rise. The number of diabetic patients is expected to cross 400 million [2] and the total worldwide health expenditure for diabetes is estimated to be in excess of US$560 billion per year by 2030 [3]. This shows how much of an economic burden diabetes poses to be for national healthcare systems globally. *Diabetes mellitus* is broadly categorised into the three most common types – type 1, type 2, and gestational diabetes.

Type 1 diabetes, formerly known as juvenile diabetes, is usually diagnosed in children and young adults, although it can appear at any age. It accounts for 10% of all diabetes mellitus cases. Type 1 diabetes is the result of insulin deficiency in the body which is caused by an autoimmune condition in the affected individuals, whereby insulin-producing β-cells in the pancreas are destroyed by T-cells, eventually leading to hyperglycaemia [4]. People with type 1 diabetes need to take insulin every day to stay alive.

Type 2 diabetes is often categorized as a 'lifestyle disease' and manifests as a result of the body's inability to effectively utilise insulin (insulin resistance) and lack of insulin production, leading to high blood glucose levels. This form of diabetes is often associated with lack of physical activity and obesity [5]. For

type 2 diabetes, initial treatment focuses on delaying disease progression via exercise and control of meals. Furthermore, patients are prescribed oral and/or injectable medications to improve their insulin production and function. However, insulin is required as the body's own insulin production diminishes eventually.

Gestational diabetes develops in some pregnant women, however, most of the time, this type of diabetes goes away after the baby is born. People with gestational diabetes have a greater chance of developing type 2 diabetes later in life. Sometimes diabetes diagnosed during pregnancy is actually type 2 diabetes.

1.2. Clinical manifestations of diabetes

Typical symptoms of diabetes are listed as follows:

- Increased frequency of urination
- Excessive thirst
- Extreme hunger – even though patient is having sufficient food
- Feeling very tired all the time
- Cloudy vision
- Slow healing of minor injuries
- Unexplained weight loss even though patient is eating more
- Tingling or numbness in the hands and/or feet

Some people may experience only a few of the symptoms listed above. A lot of people with type 2 diabetes experience very mild to no symptoms and hence remain incognizant of their medical condition.

1.3. Insulin

It is a 51-amino acid polypeptide hormone produced by the ß-cells of the islets of Langerhans in the pancreas. The amino acids are distributed in two chains of 21 and 30 amino acids. The chains are linked together by two disulphide bridges. Insulin controls the glucose levels in blood by inducing the liver and muscle cells to take up glucose from the blood [6]. In type 1 diabetes, an autoimmune response causes the destruction of ß-cells by T-cells which leads to insulin deficiency and high blood glucose levels. Insulin, like other proteins and peptides, is unstable in the gastrointestinal tract and hence oral delivery is not feasible. Consequently, subcutaneous injections of insulin are used [7]

1.4. Current treatment options for diabetes

Early detection and treatment of diabetes can reduce the risk of developing the complications of diabetes. Maintenance of continuous normoglycaemic conditions (70–140 mg per dl or 4–8 mM of glucose) is the key goal for the management of both type 1 and type 2 diabetes in patients [8]. This level of glucose is currently managed by subcutaneous injections, usually by the patients themselves or by trained professionals. Hyperglycaemia (high blood glucose levels), if left untreated for a prolonged period of time, can lead to medical complications such as blindness, heart and kidney failure, nerve degeneration, and foot ulceration leading to amputation [9]. Contrarily, an excess of insulin in blood can lead to hypoglycaemia (low blood glucose levels) which can result in seizures, unconsciousness or even death [10].

Insulin replacement therapy is prescribed for the management of Type 1 diabetes [11]. For type 2 diabetes, lifestyle changes and oral medications are the initial

modes of treatment to improve insulin production and function [1]. However, as the body's natural insulin production gradually declines, insulin replacement therapy is eventually necessary to control blood glucose levels [6]. Typical insulin treatment involves injections of fast-acting insulin during mealtimes, followed by longer-acting insulin injections which maintain a baseline insulin level throughout the day [11,12].

Subcutaneous injections of insulin are painful and cumbersome leading to poor patient compliance. Furthermore, this form of insulin therapy is 'open-loop', which means that the insulin doses are determined by the history of the patients' blood glucose profile after various meals and insulin treatments [13]. All these make it extremely difficult to maintain ideal blood glucose levels throughout the day. Future insulin therapies need to be glucose-regulated, less painful, relatively inexpensive to manufacture and easily available for administration in clinical settings [14]. Currently, scientists are working towards achieving these goals by exploring other routes of insulin delivery [15], modulating the pharmacokinetics of insulin [11] and formulating other therapeutics [16].

1.4.1. Improved technologies for insulin replacement therapy

Several technologies have recently been developed to overcome the above-mentioned challenges of insulin replacement therapy. Pickup reported an insulin pump which can be worn externally and is composed of an insulin depot connected to a subcutaneously implanted cannula. The depot can be replaced when necessary and the pump can be adjusted to deliver both a bolus dose of insulin for mealtimes, and a basal dose throughout the day [14]. Another recent invention is the microcomputer-programmed insulin pump that comes with a

continuous glucose monitor (CGM) [17]. The CGM, which is linked directly to the pump, can be used to calculate the correct insulin dosage. The pump can then inject the required amount of insulin, thus providing a glucose-dependent insulin delivery to the patient.

Even with these innovative technologies to improve patient compliance and maintain tight glycaemic control required in patients, there are several disadvantages. The insulin pumps need to be replaced and maintained frequently for proper functioning which is costly. Furthermore, the implantation of sensors and cannulas are invasive and present the risk of infection and inflammation as the body considers these as foreign objects [14].

1.4.2. Alternative routes of insulin delivery

Oral route is the preferred route of drug delivery, however, it is not feasible to deliver protein and peptide drugs such as insulin. The bioavailability of insulin via this route is low due to its instability in acidic conditions, enzymatic degradation and insufficient permeability across the gastrointestinal mucosa [18]. As a result, researchers are exploring alternative routes of insulin delivery. Besides subcutaneous route, the intranasal and pulmonary routes are being increasingly investigated.

The nasal cavity has a large surface area-to-volume ratio for absorption of drugs. Furthermore, the high vascularity of the nasal mucosa means that the absorbed drugs are rapidly cleared from the site of absorption. This ensures fast and direct entry of drugs into the systemic circulation, avoiding the hepatic first-pass metabolism [19]. Despite the potential of the nasal route, there are a number of factors that limit the efficient absorption and systemic delivery of peptide drugs.

Continuous mucociliary clearance, presence of proteolytic enzymes and low permeability of the nasal epithelia are the main constraints that limit the systemic bioavailability of insulin following intranasal administration [20,21].

The respiratory tree offers great promise as the pulmonary route for insulin delivery due to its high vascularisation and large surface area. However, factors like breathing pattern, lung disease, smoking, and patients' ability to use inhalation devices might limit the efficient systemic delivery of insulin.

1.5. Nanotechnology in medicine

In the last two decades, advances in nanotechnology have vastly improved both diagnosis and treatments in the field of cancer and cardiovascular biology [22-25]. Various nanoparticulate formulations such as liposomes, polymer nanoparticles, nanostructures, metallic nanoparticles and stimuli-responsive nanoparticles have proved to be not only biocompatible but also possess ideal physicochemical properties for potential biomedical applications [26-30]. Using nanotechnology, drugs can be delivered to the site of action only. In this technique, nanoparticles containing the active medicinal ingredient release the drug at the morbid region only, hence reducing systemic side-effects and also the cost of treatment. Nanoparticles can also be modified to encapsulate artificial cells which can be used in tissue engineering to repair damaged cells or organs in the body.

1.5.1. Diabetes management with nanotechnology

In the recent past, scientists have started exploring the potential of nanotechnology for diagnosis, monitoring and treatment of diabetes. Progress in

the field of nanotechnology and polymer science can now enable scientists to engineer nanoparticles that can release the loaded drug by sensing changes in their surroundings [13]. We believe that this would stage the new frontier in management of diabetes, taking into account most of the drawbacks associated with the current mode of administration as well as the challenges posed when considering alternate routes of administration. Whilst we are still very far off, a system capable of releasing insulin in response to an increase in blood glucose concentration presents the closest we can get in designing an artificial pancreas.

1.6. Glucose responsive insulin delivery (GRID)

GRID is a method whereby insulin is released in response to a rise in blood glucose levels and the release is stopped when blood glucose goes back to euglycaemic levels. These systems have the potential to act as artificial pancreas as they can modulate the insulin release relative to external glucose concentrations, hence simulating the body's natural physiological response to changes in blood glucose levels. Consequently, these 'closed-loop' systems can not only achieve tighter glycaemic control by preventing both hypo- and hyperglycaemia, but also eliminate the need for frequent finger-stick glucose tests and multiple daily insulin injections [31]. Currently, the three most extensively studied glucose sensors are glucose oxidase, glucose-binding proteins and glucose-binding small molecules. Using these glucose responsive molecules, insulin loaded nanoparticles can be formulated which will release the drug via degradation, disassembly or swelling in response to changes in blood glucose concentrations [32,33].

1.6.1. Glucose oxidase

It is an enzyme that converts glucose to gluconic acid in the presence of oxygen (fig.1.1) and is currently the most widely studied glucose sensor in the literature. An early example of the potential use of glucose oxidase for GRID dates back to 1988 when Fischel-Ghodsian et al. formulated insulin analogues which were soluble in acidic pH but insoluble in pH 7.4 (physiological conditions). When implanted in the body, high blood glucose levels resulted in acidic conditions surrounding the system leading to the release of insulin [34]. More recently, Gu et al. have demonstrated insulin release and control of blood glucose in animal models from a microgel GRID composed of chitosan, glucose oxidase nanocapsules and insulin [35]. Qi et al. and Luo et al. have developed insulin containing polymeric nanoparticles that release the drug in acidic conditions [36,37]. While glucose oxidase-based systems boast being highly specific, their response can sometimes be slow or irregular due to changes in environmental temperature and oxygen concentrations.

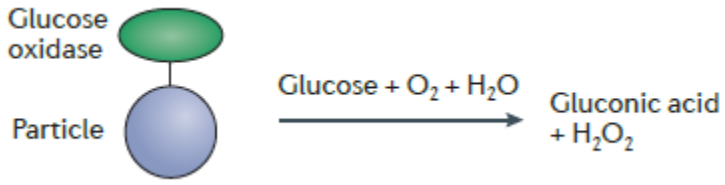

Fig.1.1. Glucose oxidase-based sensor [13]

1.6.2. Glucose-binding protein (GBP)

GBP is an alternative to non-enzymatic GRID. The proteins can be used to crosslink polymer chains together to form nanoparticles. Interaction between glucose and the proteins results in destabilisation of the nanoparticles and the

loaded drug can be released via disassembly or swelling. Brownlee et al. demonstrated such a system using the glucose-binding lectin, ConA (fig.1.2) [38]. As glucose-binding proteins possess high affinity and specificity for glucose, they have continued to gather increasing attention as potential for GRID system. However, immunological response to foreign ConA has been the major issue that needs to be overcome for their clinical use [39].

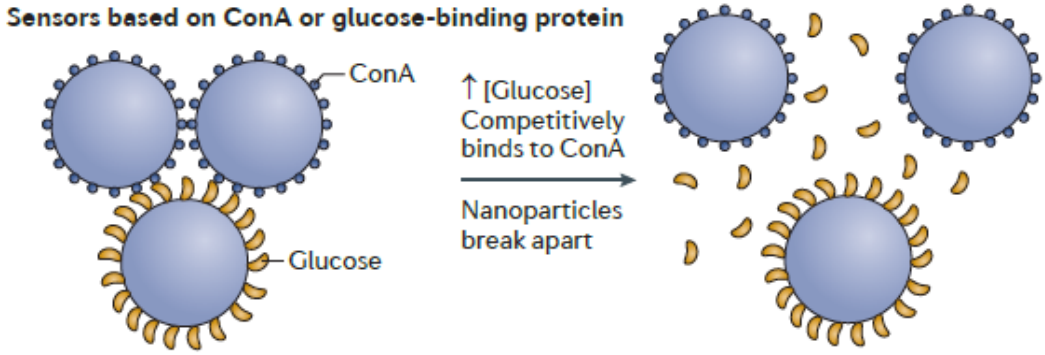

Fig.1.2. GBP-based sensor[13]

1.6.3. Boronic acids

Small molecule glucose binders such as boronic acids offer a completely different approach to glucose-mediated insulin release. Phenylboronic acids, for instance, can be conjugated to or crosslinked between suitable polymers which can then be formulated into insulin-loaded nanoparticles. Interaction between glucose and boronic acid at high blood glucose concentrations will result in swelling of the nanoparticle matrix leading to insulin release (fig.1.3). When the blood glucose level goes back to normal, the interaction is reduced and the swelling is minised and hence the insulin release. While this chemical system offers the advantage of having fast response rates and no immunological response, it lacks in specificity as boronic acids can interact with other diols (fructose, in

particular) in blood. Research is underway to improve the sensitivity of boronic acids to glucose [13].

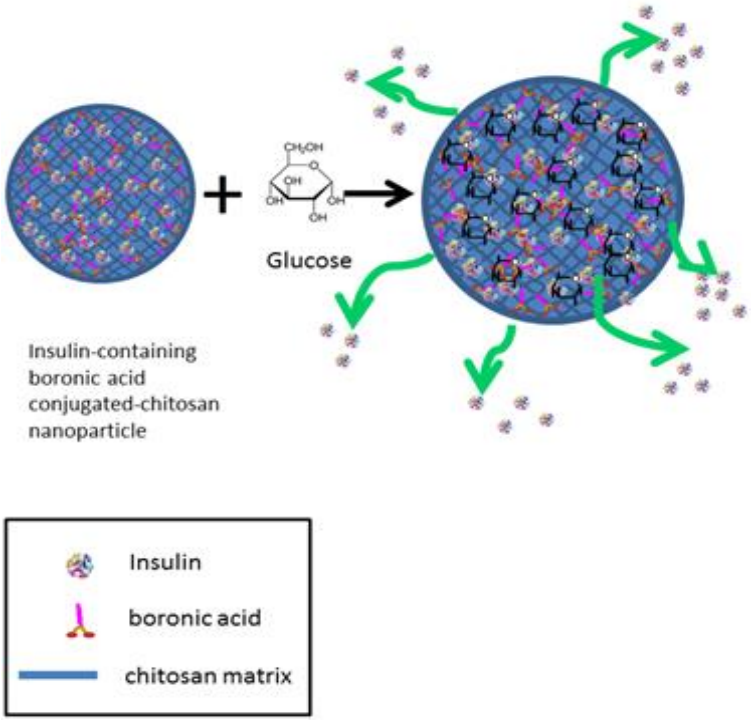

Fig.1.3. Boronic acid-based sensor

1.7. Polymer-based nanoparticulate insulin delivery systems

Evolution in the field of polymer science and drug delivery in the last decades have led to better understanding of polymer structure and improved polymeric drug delivery systems. In this regard, biodegradable and biocompatible polymers serve an added advantage when used in conjunction with drug delivery. Different methods and technologies can now be used to prepare polymeric nanoparticles depending on the required physicochemical properties for targeted drug delivery. Several polymers – both natural and synthetic – have been used to prepare insulin loaded nanoparticles for its efficient delivery [40]. An outline of the more commonly used polymers in nanodrug delivery follows.

1.7.1. PLA nanoparticles

Poly(lactic acid) (PLA) is a synthetic polyester polymer that is considered biocompatible and biodegradable due to the hydrolysis of its monomeric units in the body [40]. Xiong et al. developed a pluronic block copolymer (PLA-b-pluronic-b-PLA) vesicles for oral delivery of insulin [41]. The *in vitro* release study showed a biphasic release profile of insulin from their vesicles. *In vivo* investigation using diabetic mice revealed extended hypoglycaemic effects of the insulin vesicles which showed promise to be developed into an orally administered formulation. In a more recent study, the same group proved the biocompatibility of their vesicles using human ovarian cancer cells [42].

1.7.2. PLGA nanoparticles

Poly(lactic-co-glycolic acid) (PLGA) is an aliphatic copolymer that has been widely investigated for drug delivery in general. For example, it has been used in insulin delivery due to its biodegradability, biocompatibility and prolonged-release profiles. PLGA offers additional advantage in that it can be combined with other polymers or coated with various ligands to improve encapsulation efficiency and the uptake of loaded insulin [40]. Yang et al. formulated PLGA-loaded insulin nanoparticles and found that insulin was released at a lower rate in acidic pH reaching about 90% of release in 11 days. On the other hand, the release was faster under physiological conditions since about 90% of the total amount of insulin was released in 3 days. *In vivo* studies involving oral administration of the nanoparticles to diabetic rats revealed a decrease in blood glucose levels with an increase in blood insulin levels. These results showed the extended release properties of PLGA nanoparticles, and their ability to protect

insulin and consequently decrease the blood glucose levels when administered orally [43]. However, it should be noted that PLA and PLGA nanoparticles have an overall negative charge and this property may reduce the uptake of insulin nanoparticles through the intestinal membrane, and hence decrease the bioavailability of oral formulations of insulin.

1.7.3. Dextran nanoparticles

Dextran is a polysaccharide made up of α-D-glycose units that bind to each other through glycosidic bonds. Since it is a natural polymer, it has high biocompatibility and biodegradability in the body [40]. Chalasani et al. formulated insulin containing dextran nanoparticles by an emulsion method. The encapsulation efficiency of the system was between 45 and 70% and from that, 65 to 83% of insulin remained protected from the grastrointestinal proteases. *In vitro* release experiments showed an extended release of up to 95% within 48hr, while the *in vivo* test resulted in a plasma glucose level decrease from 70 to 75% after 5hr of oral administration, reaching basal levels in 8–10hr which was then sustained for 54hr [44].

1.7.4. Chitosan nanoparticles

Among the natural polymers, chitosan is the most widely used for insulin delivery because of its high biocompatibility, biodegradability, non-toxicity and hydrophilicity. Furthermore, it is relatively simple and easy to prepare chitosan nanoparticles via dropwise addition of a suitable cross linker such as tripolyphosphate or via polyelectrolyte complexation with insulin on its own. As the nanoparticles form spontaneously in aqueous media with high encapsulation efficiency, there is no need for additional solvents or heating, hence eliminating

concerns of cytotoxicity and insulin instability. These are some of the main advantages of chitosan over other polymers [45,46]. Pan et al. proved that chitosan nanoparticles are able to enhance the intestinal absorption of insulin. The encapsulation efficiency of their nanoparticles was up to 80% and the release profile of insulin manifested an initial burst release phase which depended on the pH of the environment. When administrated *in vivo*, insulin-loaded chitosan nanoparticles resulted in hypoglycemia for 15hr with about 15% higher bioavailability of insulin compared to that after subcutaneous administration of insulin [47].

1.8. Objectives of the research

For a GRID system to present as an artificial pancreas, it should ideally be implanted only once inside the body. However, as discussed before, the current insulin pumps need frequent replenishment and hence the surgical implantation has to be carried out regularly.

In this research, we aim to formulate a GRID system that can be used to deliver substantial quantities of the drug with hopefully a lesser dosing frequency. Nanoparticles are chosen as the delivery carrier because of the high surface area-to-volume ratio, which means that the response time for the delivery of insulin when in contact with glucose is rapid. The large surface area also allows us to improve the payload. Our primary objective is to formulate a novel polymeric glucose responsive insulin-containing nanoparticulate system using boronic acid as the glucose sensor. The chosen polymer is chitosan and the boronic acid is 2-formyl-3-thienylboronic acid. It is hypothesised that the formulated GRID system can be used to deliver insulin on a repeated basis via transdermal patches, depot

injections, inhalable devices or even oral routes. This will eliminate the need for repeated invasive surgical procedures, while at the same time significantly improving overall glycaemic control of insulin therapy.

To achieve the primary goal, specific objectives that would ensure that the system functions properly are outlined below:

- To conjugate the boronic acid to chitosan
- To characterise the resulting conjugates
- To formulate the conjugates into a nanoparticulate GRID system
- To characterise the nanoparticulate GRID system
- To test the efficiency of the formulated GRID system *in vitro*

CHAPTER 2

SYNTHESIS AND CHARACTERISATION OF CHITOSAN-BORONIC ACID CONJUGATES

2.1. Introduction

The capability of boronic acids (BAs) to act as chemosensors in biological systems is evident from the increasing number of literature in this particular field of research. Saccharides are one of the primary target species for boronic acid interactions. These polyhydroxyl entities of saccharides have "high solvation enthalpies in aqueous solutions" and have little structural differences apart from their configurations which make them extremely difficult to be distinguished by most synthetic chemosensors [48]. This is one of the fundamental reasons as to why there has been very little progress in the development of glucose-responsive sensors past the clinical stage. As discussed in chapter 1, glucose oxidase and glucose-binding proteins such as lectins are currently being widely investigated for their potential use as glucose sensors. Notwithstanding, unlike biological sensors, synthetic sensors are cheaper, more stable and oxygen-independent which makes them more attractive. Boronic acids (BAs) are promising candidates as synthetic sensors for glucose detection [48].

BAs bind reversibly to *cis*-1,2- or 1,3-diols via covalent interactions to form five- or six-membered cyclic esters. The interaction has been proven to be so strong that mM or even sub-mM levels of saccharides in biological systems can bind to boronic acids. BAs can distinguish between different saccharides as the strength

of binding depends on the positions of the hydroxyl groups. It has now been shown that monoboronic acids have the highest selectivity for fructose among all the saccharides [49]. This is because the ß-D-fructofuranose (fig.2.1a) is the form of fructose that binds to boronic acids and is available as 25% of total fructose in D_2O at 31°C. On the other hand, with glucose, the α-D-glucofuranose (fig.2.1b) form that binds to boronic acids makes up only 0.14% of the total glucose in D_2O at 27°C [48].

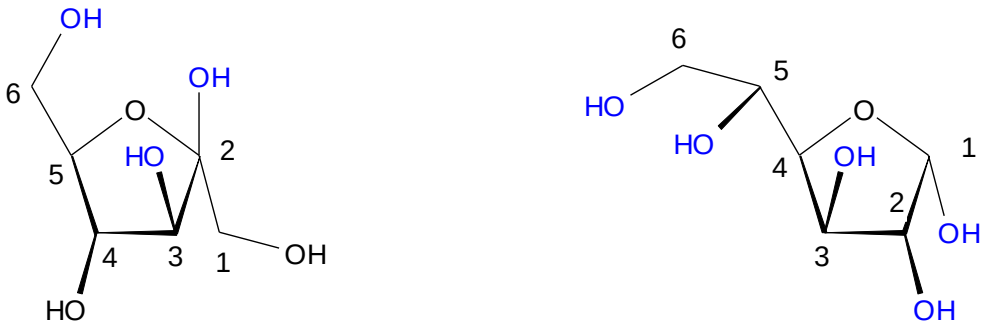

(a) (b)

Fig.2.1. Structures of (a) fructose and (b) glucose that take part in interaction with boronic acids in solution; potential boronic acid binding sites are highlighted in blue

This poses a problem for monoboronic acids to act as glucose-specific sensors for systemic insulin delivery because blood has both glucose and fructose and insulin release due to the presence of fructose is undesirable in the present context. However, the problem can be overcome by using properly positioned multiboronic acids. The use of multiboronic acids for glucose-specific response is similar to the way biological sensors like lectins work as they have multiple binding sites. Multivalency, in chemistry and in biological systems, is a key concept which means that when two multivalent (i.e. having more than one

binding site) moieties are involved in *n* binding events (*n* > 1), the binding occurs with higher affinity than the sum of *n* individual monovalent bindings. According to fig.2.1, fructose has one binding moiety while, glucose has two (at the 1,2- and 3,5,6-positions). Consequently, monoboronic acids with one binding moiety interact with greater affinity with fructose since monovalent interactions take place here. However, in di- or multiboronic acids, there are at least two boronic acid moieties available for interaction with one glucose molecule, and hence this interaction is substantially stronger than monovalent interactions which take place with fructose [48].

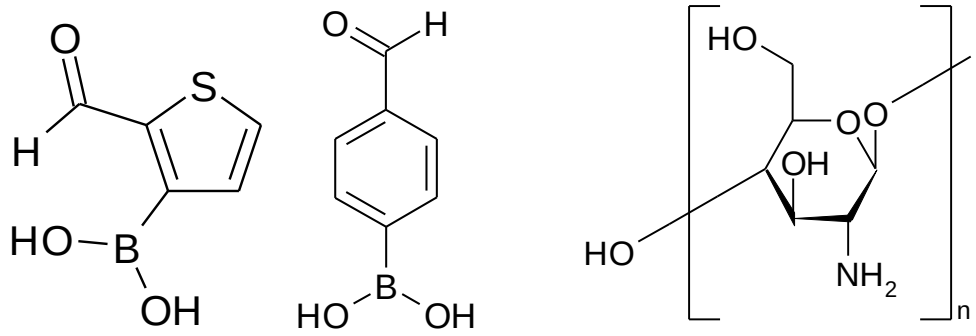

(a) (b) (c)

Fig.2.2. Structures of (a) FTBA, (b) FPBA and (c) chitosan

Over the last ten years, scientists have proposed several methods to develop glucose-specific boronic acid-based sensors using this concept of multivalency. Currently, four main strategies are being widely investigated which include synthetic diboronic acids, boronic acid-conjugated polymers, self-assembly of simple boronic acids and boronic acid-conjugated nanomaterials [48]. In this project, we focus on the covalent attachment of boronic acid to a polymer and use this multiboronic acid scaffold as a glucose-specific sensor. We report for the first time the use of 2-formyl-3-thienylboronic acid (FTBA) (fig.2.2a) as the

boronic acid to be conjugated to a polymer to develop a chemosensor. The polymer used is chitosan (fig.2.2c) and the organic reaction used to conjugate the boronic acid to chitosan is reductive N-alkylation (fig.2.3). Asantewaa et al. used 4-formylphenylboronic acid (FPBA) (fig.2.2b) to prepare chitosan conjugates [50] and since it has the same functional group involved in the reductive N-alkylation method as FTBA, FPBA was also used in this investigation for comparison. The conjugates were extensively examined via various spectroscopic methods for evidence of the functionalisation of the BAs to chitosan and eventually tested for their glucose specificity.

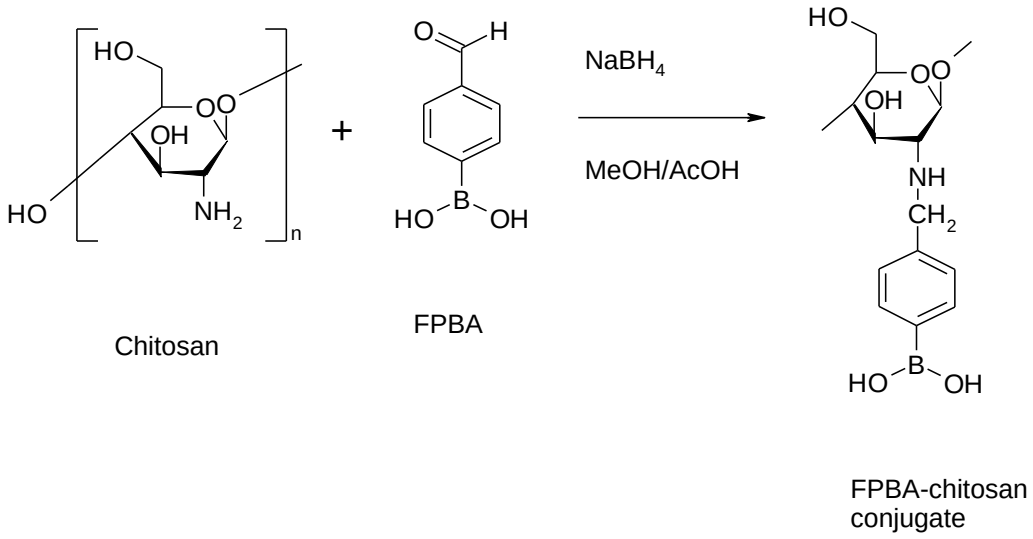

Chitosan

FPBA

FPBA-chitosan conjugate

(a)

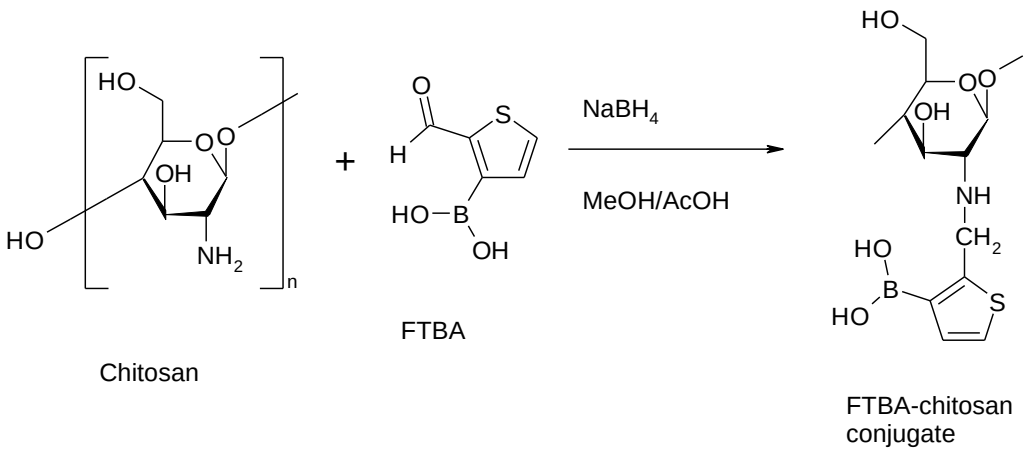

(b)

Fig.2.3. Reductive N-alkylation between chitosan and (a) FPBA and (b) FTBA

2.2. Materials and methods

2.2.1. Materials

Low molecular weight chitosan, 4-formylphenylboronic acid, 2-formyl-3-thienylboronic acid, sodium borohydride, glucose hexokinase assay kit and curcumin were purchased from Sigma Aldrich (St. Louis, MO, USA); acetic acid, methanol, acetonitrile, fructose and glucose were purchased from Thermo Fischer Scientific (Bridgewater, NJ, USA). All other chemicals were of reagent grade.

2.2.2. Synthesis and purification of boronic acid-chitosan conjugates

50mg of chitosan (dissolved in 1% acetic acid) and various molar equivalents of FPBA and FTBA (Table 2.1) were mixed and stirred in separate clean beakers containing 15mls of methanol. After 3 hours, sodium borohydride (1.6 x the molar

equivalences of FPBA and FTBA) was added in respective beakers and the mixtures were allowed to stir for a further 10 minutes. Afterwards, the reaction was quenched with 1M sodium hydroxide. The precipitates formed were centrifuged at 1610g for 10mins and washed thoroughly with methanol, ethanol and water to remove any unreacted BAs. The conjugates were then lyophilised and stored in 2^{o}C for use in further studies.

	Boronic acid:chitosan				
	0.5:1 (F1)	**1:1 (F2)**	**1.5:1 (F3)**	**2:1 (F4)**	**3:1 (F5)**
Chitosan (mg)	50				
FPBA (mg)	23.3	46.6	69.9	93.2	139.8
FTBA (mg)	24.2	48.4	72.6	96.8	145.2
$NaBH_4$ (mg)	9.4	18.8	28.2	37.6	56.4

Table 2.1. Variations of FPBA and FTBA used to formulate conjugates

2.2.3. Fourier transform infrared spectroscopy (FTIR) analyses

The FTIR spectra of pure chitosan, FPBA- and FTBA-chitosan conjugates were obtained via a Perkin Elmer FTIR Spectrometer (RX1 S/N 74041, US). Freeze-dried conjugates were mixed with KBr at a ratio of 1:99 and the mixture ground to fine powder using a mortar and pestle. The powder was compressed into a disc at 5000 psi for 5 min using a pneumatic press and infra-red spectra collected in the range of 2000-400 cm^{-1}.

2.2.4. Differential scanning calorimetry (DSC) analyses

The DSC thermograms were obtained using a Mettler Tolledo DSC (UK) system. About 5 mg of freeze-dried conjugate was placed in the sample pan, while, the reference pan was a standard aluminum pan. Both sample and reference pans

were heated from 25ºC to 350ºC at a heating rate of 10ºC/min under 20 mL/min purge of nitrogen gas.

2.2.5. Glucose adsorption studies

Besides FTIR and DSC, HPLC analyses were carried out to confirm the conjugation of BAs to chitosan through glucose adsorption estimation. It is an indirect method that relies on the principle of glucose-boronic acid interaction. Pure chitosan will adsorb very little to no glucose, however, boronic acid conjugated chitosan will adsorb glucose due to the interactions between boronic acid and the hydroxyl moieties of glucose. In this investigation, 10mg of pure chitosan (control) and 10mg of the various ratios of conjugates were exposed to 1ml of 5mg/ml glucose solution (prepared with milli-Q water, pH 5.5) in eppendorf tubes separately. The tubes were placed in an incubator shaker at 100rpm and 37ºC for 1hr of equilibration. Afterwards, the mixtures were centrifuged at 4472g for 2mins and the supernatants collected to determine the amount of glucose present via HPLC. The amount present in the supernatant subtracted from the original amount present in the tubes would give the amount of glucose adsorbed by the conjugates. Since two different boronic acids are investigated in this project, this analysis will also give an indication of the extent of selectivity between the two types of conjugates for glucose.

It is extremely challenging to directly determine glucose via UV-spectroscopy hence glucose hexokinase reagent was used for an indirect estimation. In this reaction, glucose hexokinase phosphorylates glucose to glucose-6-phosphate (G6P) which in turn is oxidised to 6-phosphogluconate (6PG) by glucose-6-phosphate dehydrogenase (G6PD). During the latter reaction, NAD^+ is reduced to

NADH which can be determined via UV-spectroscopy at 340nm. Since the amount of NADH produced is directly proportional to the amount of glucose used for the entire reaction, the hexokinase assay can give us an estimate of the amount of glucose adsorbed by the conjugates. The following reactions summarise the events that take place during the hexokinase assay:

$$\text{Glucose} + \text{ATP} \xrightarrow{\text{Hexokinase}} \text{G6P} + \text{ADP}$$

$$\text{G6P} + \text{NAD}^+ \xrightarrow{\text{G6PD}} \text{6PG} + \text{NADH} + \text{H}^+$$

HPLC analysis was carried out by first preparing six different standard solutions of glucose ranging from 0.25 – 10mg/ml. 10μl of each of the glucose solutions was mixed with 1ml of hexokinase reagent (in excess) in HPLC vials. The parameters for the HPLC analysis are as follows:

- mobile phase – 20mM potassium dihydrogen phosphate and acetonitrile in the ratio 95:5
- elution – isocratic with a flow rate of 1ml/min
- injection volume – 20μl
- detection wavelength – 340nm
- column – Phenomenex Jupiter® C_{18} with with particle size of 5 μm and pore size of 300Å

A calibration curve of average peak area against glucose concentration was plotted and the R^2 value and the equation of the line determined. To calculate the glucose adsorption of the conjugates, 10μl of the supernatant from the samples were equilibrated with 1ml of hexokinase and the above procedure was followed to determine the absorbance.

2.2.6. Investigation of boronic acid selectivity for diols (glucose and fructose)

The affinities of the two boronic acids for glucose and fructose were studied using a different HPLC analysis. This is an indirect but a novel way of determining the selectivity of the conjugates for the diols. Springsteen et al. used a dye called Alizarin Red S (ARS) to determine the affinities of PBA for various diols [51]. In this project, curcumin was used as the dye for the same purpose. The method is based on the premise that curcumin reacts with boronic acids in solution to form a complex called rosocyanine (fig.2.4).

Fig.2.4. Rosocyanine complexes of varying boronic acid concentrations

During this reaction, the colour changes from yellow (curcumin) to bright red (rosocyanine) and both the colour intensities can be determined spectrophotometrically [52]. In this project, 10mg of the conjugates (ratios 1:1, 2:1 and 3:1) were equilibrated with 1ml of 2mg/ml glucose and fructose solutions in eppendorf tubes placed in an incubator shaker at 100rpm and 37ºC. There were also control tubes that had the conjugates exposed to 1ml of milli-Q water only. After 1hr, 500µl of 0.1mg/ml curcumin solution (dissolved in methanol) was

added in each of the tubes and shaken gently for a few seconds. The following reactions summarise the events that take place after addition of curcumin:

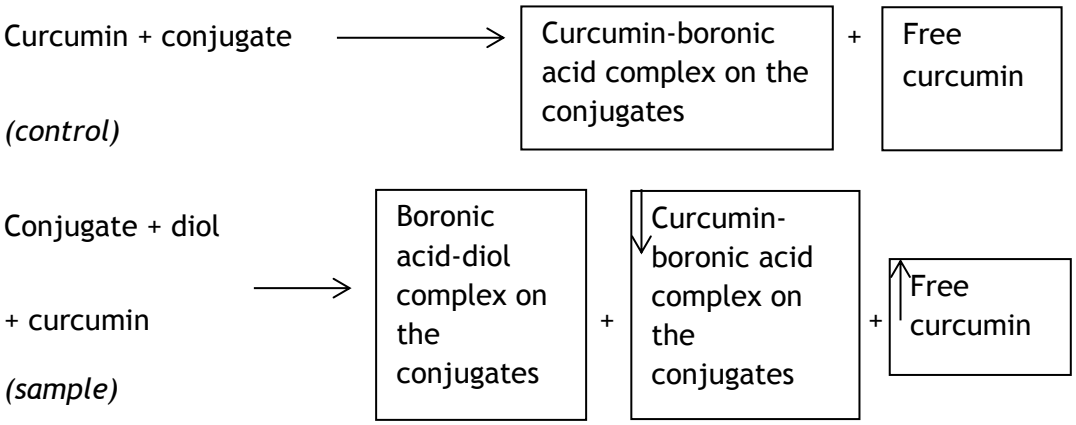

In the control, where curcumin is added after exposure of the conjugates to milli-Q water only, curcumin interacts with all the available boronic acid moieties on the solid conjugates at the bottom of the tube. Since curcumin is present in excess, there is always free curcumin in solution. In the sample tubes, where the conjugates have been equilibrated with glucose or fructose, boronic acid moieties interact with the diols with affinities of varying degrees. Consequently, fewer boronic acid moieties are available for interaction with curcumin. This also means that if the same amount of curcumin (as that in control) is added to the sample tubes, the amount of free curcumin in solution will be more in the sample tubes. Since curcumin can be detected via UV-spectroscopy at 425nm, the difference in the absorbance between the two respective 'free curcumin' solutions will give an indication of the degree of affinity of the conjugates for the two diols. This procedure has not been reported elsewhere.

The HPLC analysis was carried out by first preparing five standard solutions of curcumin ranging from 1 - 50μg/ml. The parameters for the HPLC analysis are as follows:

- mobile phase – acetonitrile, 0.01% acetic acid and methanol in the ratio 53:42:5
- elution – isocratic with a flow rate of 1.5ml/min
- injection volume – 10μl
- detection wavelength – 425nm
- column – Agilent Zorbax 300SB-4.6 x 250 mm C_{18}, with particle size of 5 μm and pore size of 300 Å

A calibration curve of average peak area against curcumin concentration was plotted and the R^2 value and the equation of the line determined. To calculate the absorbances of 'free curcumin' with and without the presence of diols, the mixtures were centrifuged at 8765g for 2mins and 10μl of the supernatants were injected into the HPLC system.

2.2.7. Statistical Analysis

A simple two-tailed t-test was performed with 95% confidence interval to check for significant differences between experimental results where necessary.

2.3. Results and Discussion

2.3.1. Characterisation of conjugates

The conjugation of boronic acid to chitosan was confirmed via FTIR, DSC and HPLC analysis (involving glucose hexokinase reagent). Fig.2.5a and b show the FTIR spectra of FPBA- and FTBA-conjugated chitosan respectively. In both these figures, the characteristic peak for chitosan can be seen at around 1650cm^{-1}, which is attributed to an amide-linked carbonyl group. In fig.2.5a, the main focus should be at the two circled ranges. For pure chitosan, a faint peak can be seen

at around 1590cm^{-1}, which is due to the presence of primary amines. However, this peak is absent in the spectra of the conjugates, meaning that the bonding of boronic acid with FPBA occurs at the primary amine position of the chitosan. Another peak which confirms the functionalisation of boronic acid to chitosan is that around 830cm^{-1}. This peak manifests when a *para*-substituted benzene ring is involved. Pure chitosan has no such structure, however pure boronic acid does and since, the conjugates show peaks at this 830cm^{-1} region of their spectra, the conjugation of boronic acid to chitosan is confirmed [50].

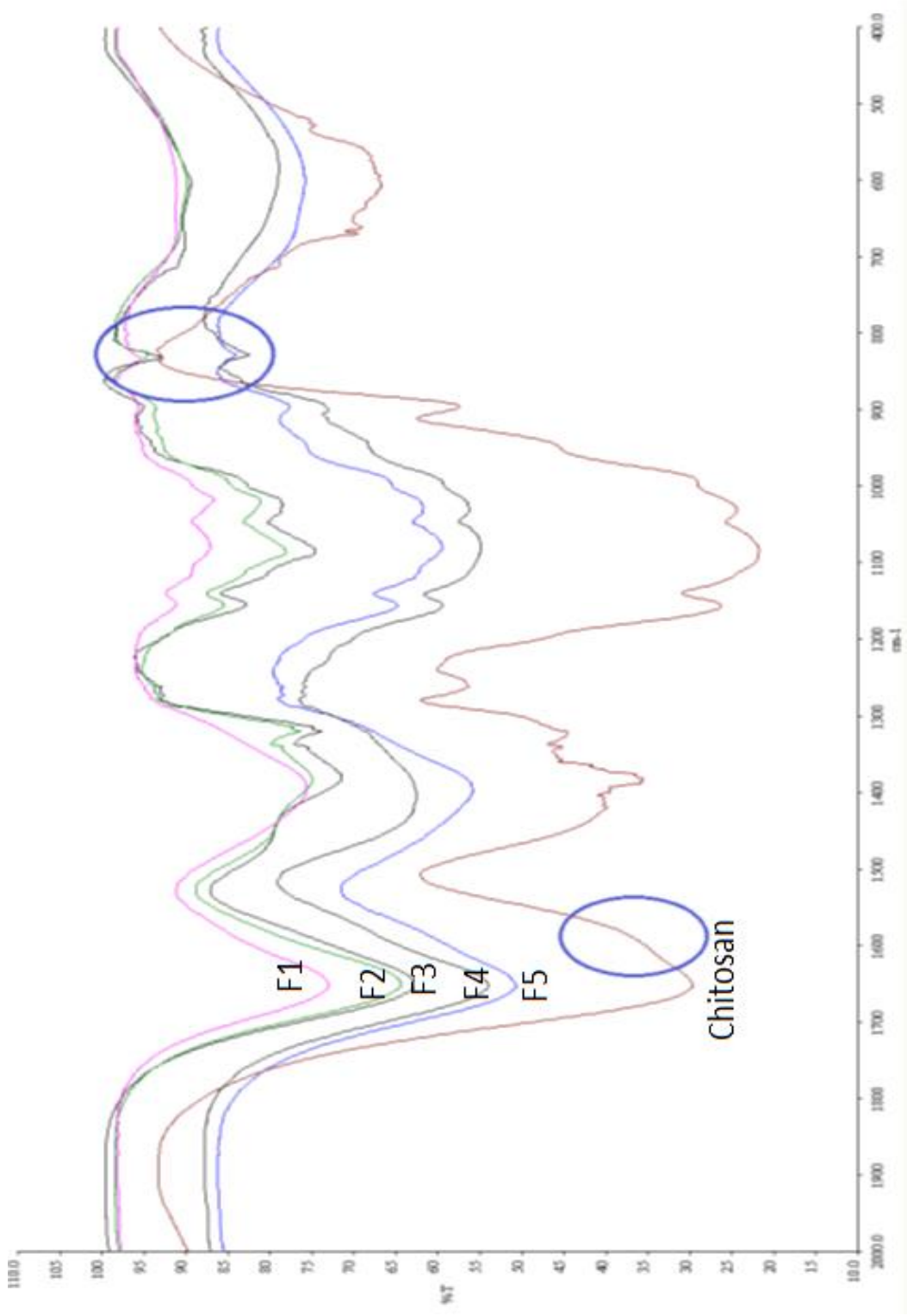

(a)

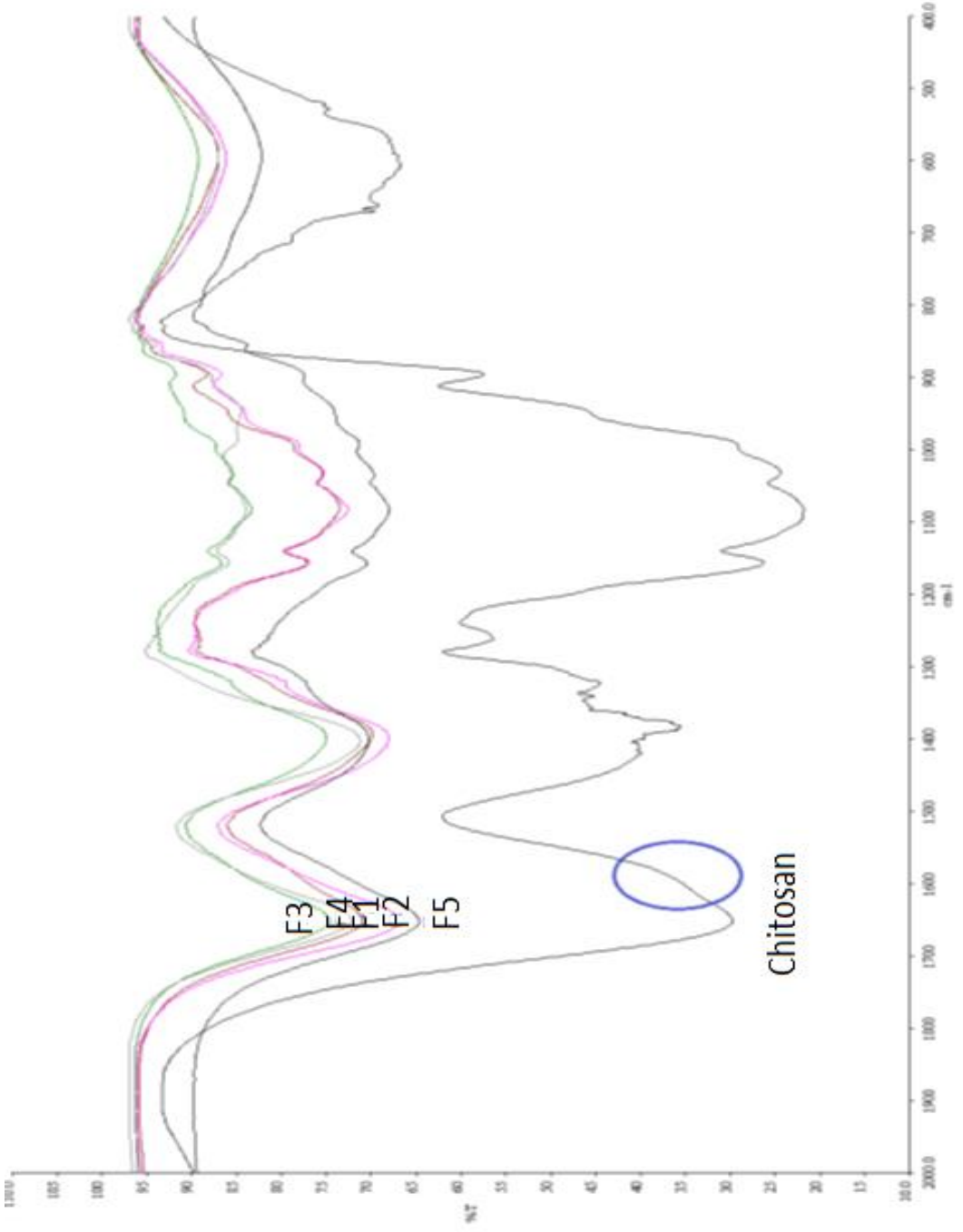

(b)

Fig.2.5. FTIR spectra of pure chitosan and (a) FPBA-chitosan and (b) FTBA-chitosan conjugates

In fig.2.5b, a similar trend in the spectra at around 1590cm^{-1} is present to prove the conjugation of boronic acid at the primary amine position of the chitosan backbone. However, no peak is present at 830cm^{-1} region of the spectra as FTBA does not have a benzene ring nor does the conjugation occur at the *para*-position of the ring.

Fig.2.6a and b depict the thermograms obtained after the DSC analyses of the FPBA and FTBA conjugates. In all the thermograms, an endothermic peak at around 100ºC is evident, which can be attributed to the liberation of water from the amine and hydroxyl groups within the chitosan backbone. Pure chitosan presents an exothermic peak at around 310ºC due to the decomposition of the primary amine group. This exothermic peak is also present in the thermograms of the conjugates, however, at progressively lower temperatures. Asantewaa et al. and Kittur et al. obtained similar thermograms and hypothesised that the lower decomposition temperature could be due to the progressive consumption of the primary amine groups as more and more boronic acids become conjugated to the chitosan backbone [50,53].

As discussed in the introduction, HPLC analysis involving glucose hexokinase was also carried out to prove the success of the reductive N-alkylation between chitosan and the two boronic acids. Fig.2.7a shows a sharp NADH peak at a retention time of around 4mins that was obtained from the HPLC analysis of one of the glucose standards. The peak is well resolved and free from interfering noise. All the glucose samples produced similar chromatograms. The calibration curve (fig.2.7b) is a straight line with a regression coefficient close to 1, indicating a strong correlation between glucose concentration and the amount of NADH produced.

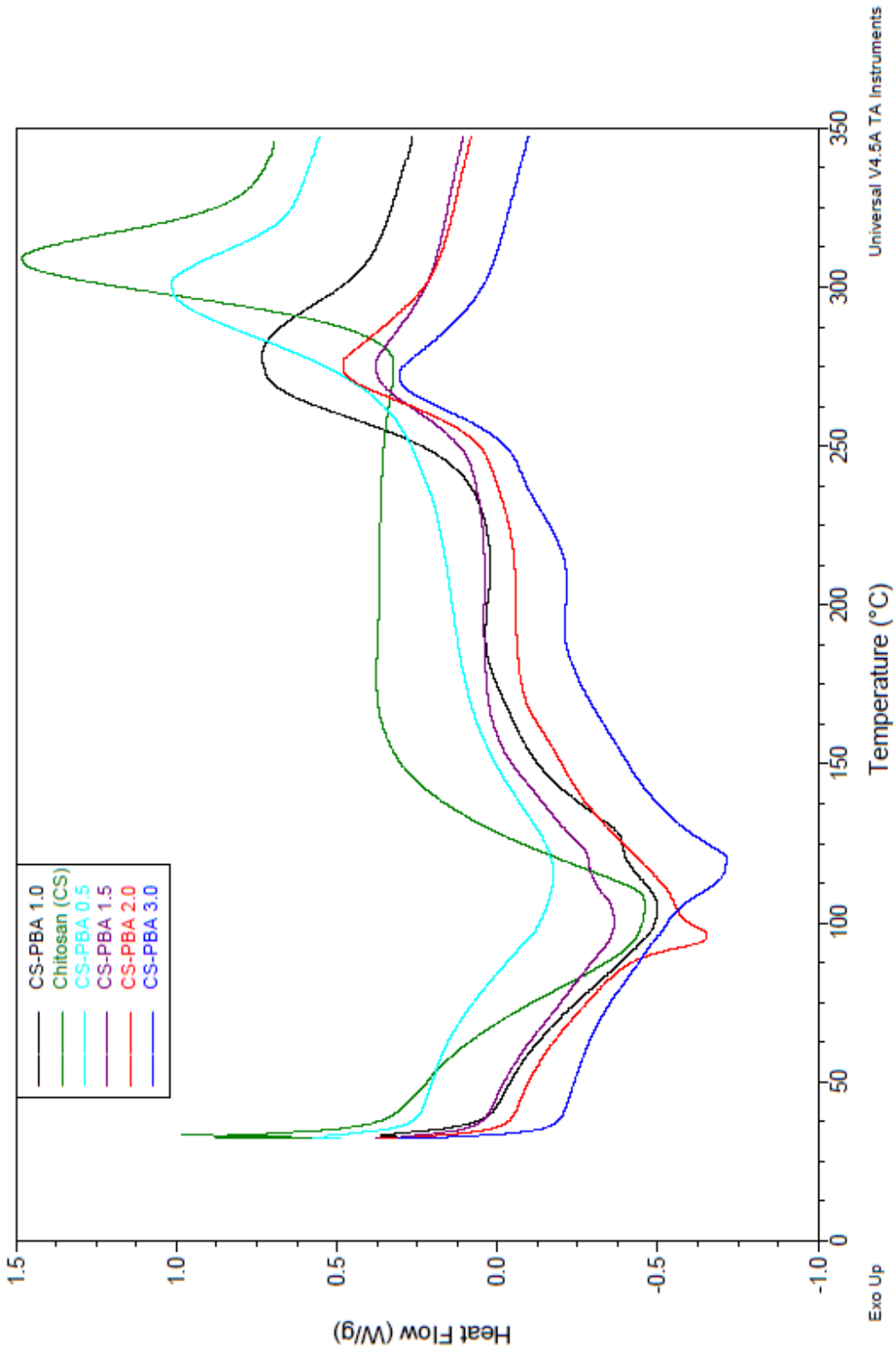
CS-PBA 1.0
Chitosan (CS)
CS-PBA 0.5
CS-PBA 1.5
CS-PBA 2.0
CS-PBA 3.0
Heat Flow (W/g)
Temperature (°C)
Exo Up
Universal V4.5A TA Instruments

(a)

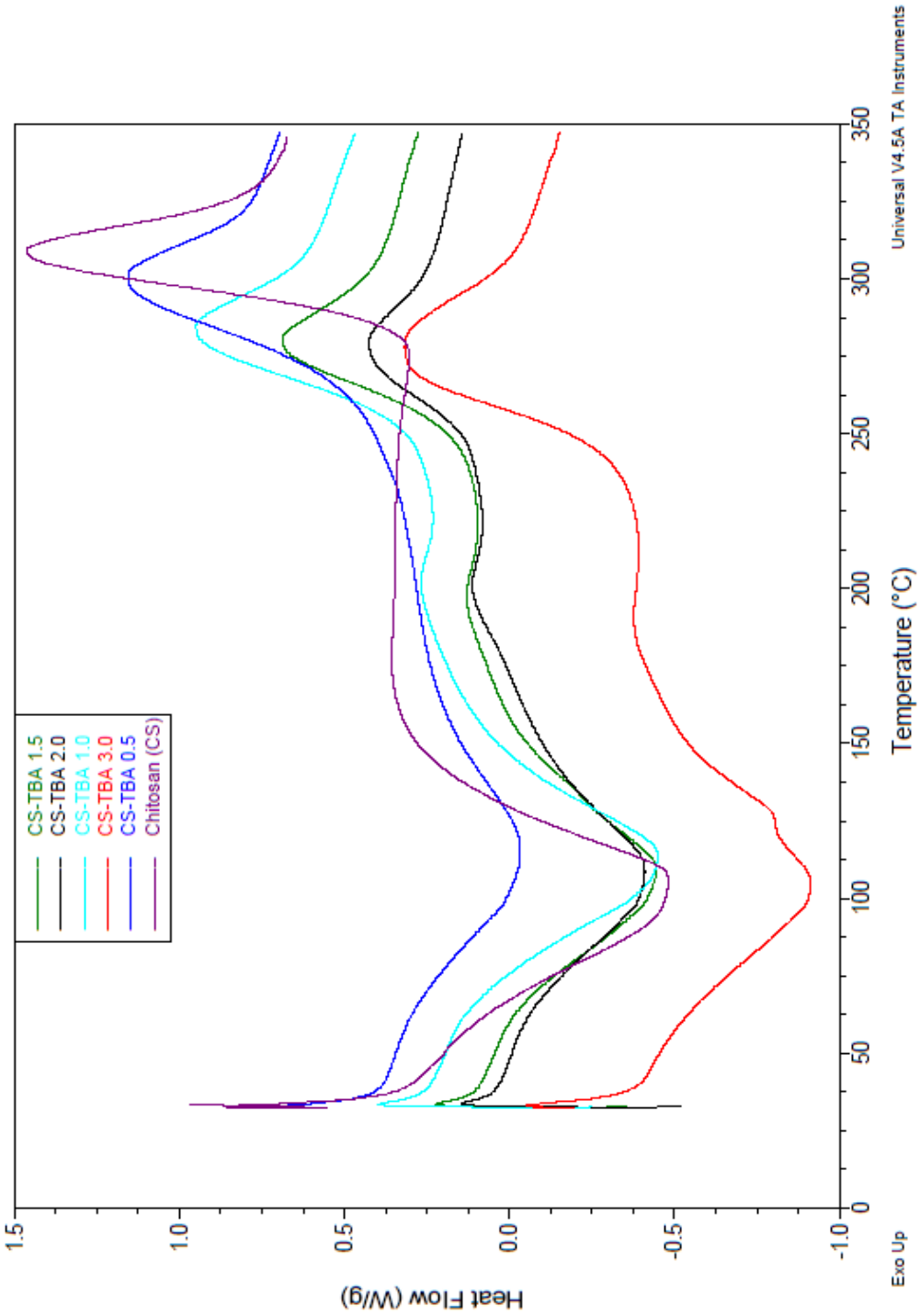

(b)

Fig.2.6. DSC thermograms of pure chitosan and (a) FPBA-chitosan and (b) FTBA-chitosan conjugates

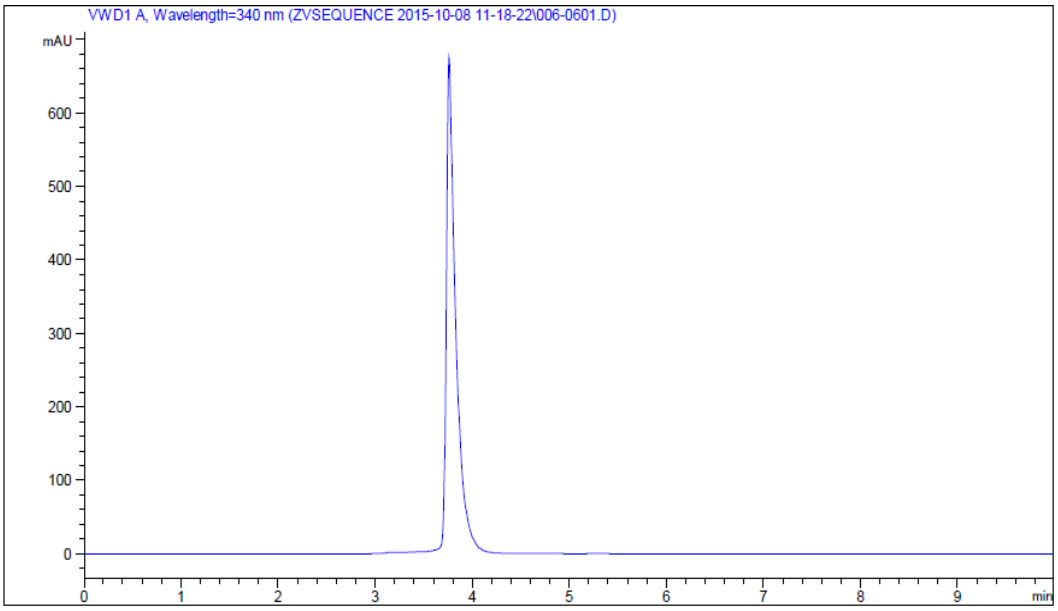

(a)

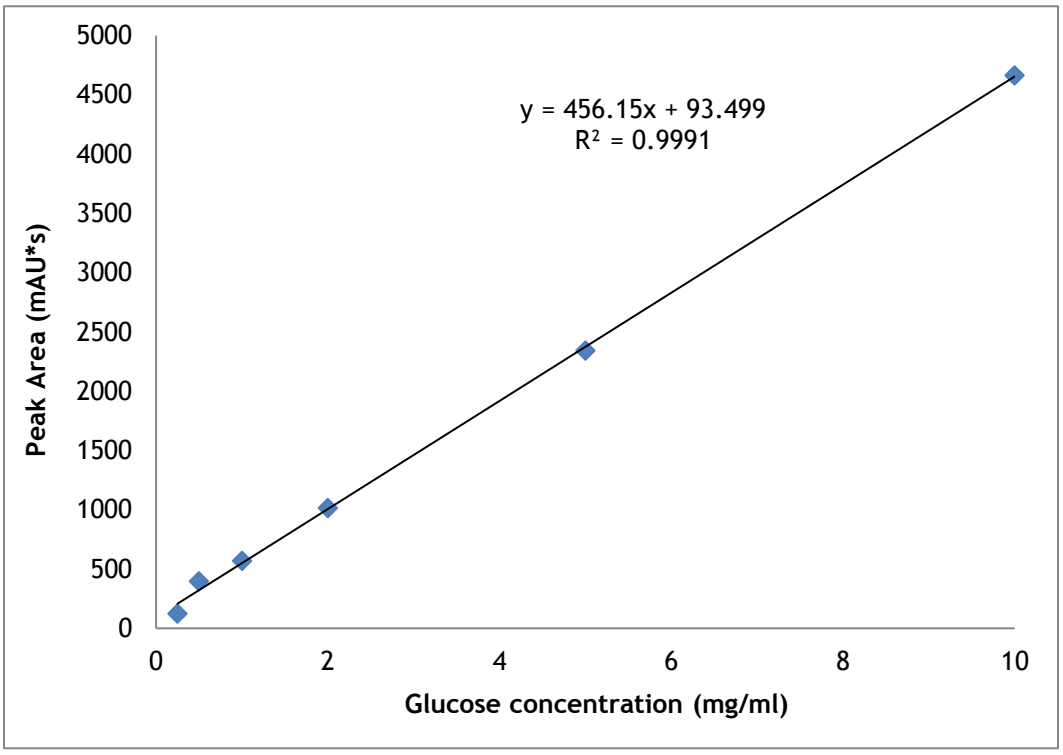

(b)

Fig.2.7. (a) Chromatogram of NADH from glucose standard (10mg/ml) and (b) Calibration curve of glucose standards

Fig.2.8 shows the percentage glucose adsorption at the various ratios of the two boronic acid-chitosan conjugates. Boronic acid is the entity that reversibly binds to glucose, hence pure chitosan adsorbs very little to no glucose. Since the conjugates have demonstrated glucose adsorption, the conjugation between boronic acids and chitosan is once again confirmed.

It can also be seen that, for both the boronic acids, as the ratio of boronic acid to chitosan increases, the glucose adsorption increases up to ratio 1:1. This result is similar to those obtained by Asantewaa et al. where they conducted their investigation using FPBA only [50]. It can be hypothesised that at ratios below 1:1, there is only an insufficient number of boronic acids attached to the chitosan backbone for glucose adsorption. At ratio 1:1, the number of boronic acids is optimum for the maximum adsorption of glucose. Interestingly, at ratios above 1:1, the number of boronic acid moieties on the chitosan backbone increases, however, this also results in an increase in the crystallinity of the conjugates [50]. Furthermore, as more and more boronic acids attach to the chitosan backbone, the close packing arrangement makes the structure increasingly rigid with increased steric hindrance to approaching diols. As the two hydroxyl moieties at 1,2- and 3,5,6-positions of α-D-glucofuranose are spread out in different directions, a flexible polymer backbone with reasonably spaced boronic acid moieties is necessary for effective multivalent binding between boronic acids and glucose [48]. This phenomenon might be one of the fundamental reasons as to why the adsorption of glucose decreases above the optimum ratio.

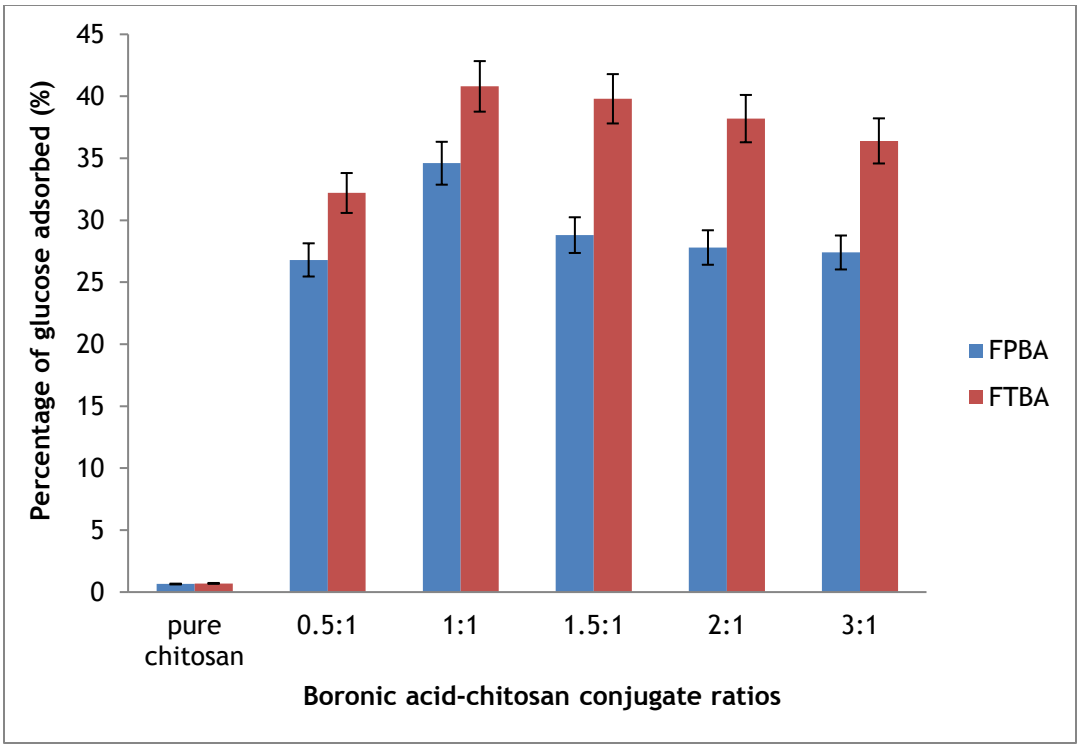

Fig.2.8. Glucose adsorption of FPBA and FTBA conjugates

It should also be noted that the FTBA conjugates (at all ratios) had a higher percentage of glucose adsorption than their FPBA counterparts (significant at all BA:chitosan ratios; $p<0.025$). In FPBA (fig.2.9a) the chitosan monomers conjugate with the boronic acids at position 4 of the phenyl ring, while in FTBA (fig.2.9b), the conjugation takes place at position 2 of the thienyl ring. Due to the proximity of the thienyl rings of FTBA and the cyclohexane rings of chitosan to the glucose molecule as it forms the complex with boronic acid, it can be postulated that additional C-H•••π interactions might contribute to a slightly higher affinity (and hence greater adsorption) of FTBA to glucose compared to that of FPBA.

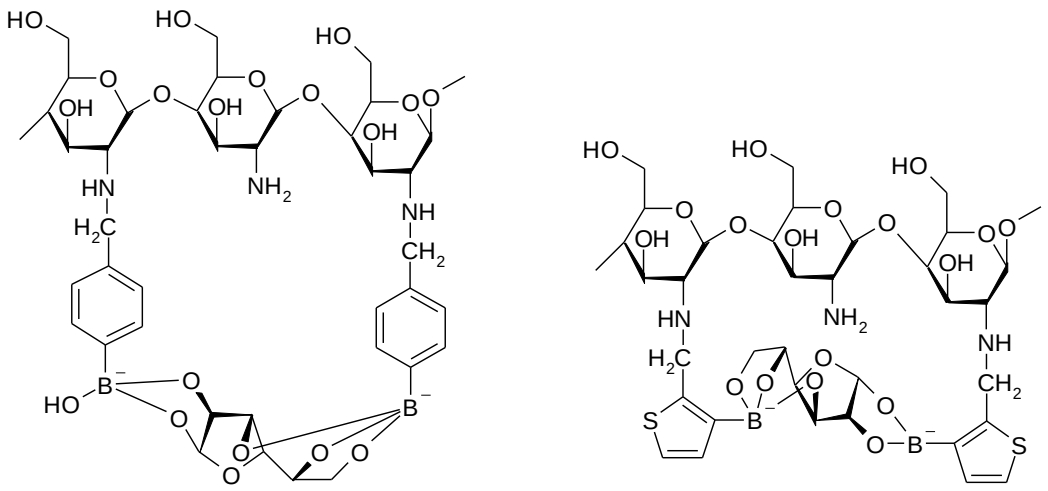

(a) (b)

Fig.2.9. Structures of α-glucofuranose complex with (a) FPBA-chitosan and (b) FTBA-chitosan conjugates

2.3.2. Selectivity of boronic acids for glucose and fructose

The idea of using curcumin to differentiate the affinities of the two boronic acid-conjugated polymers for glucose and fructose in this project was envisaged to explore a novel way of studying the kinetics of adsorption between boronic acids and diols. Curcumin can be used to detect boron even at very low (ppm) levels [52], so the slightest changes in boronic acid concentrations due to complexation between glucose and fructose can be determined using this dye. Fig.2.10a and b depict the chromatogram obtained from the HPLC analysis of a curcumin standard and the calibration curve of the standards respectively.

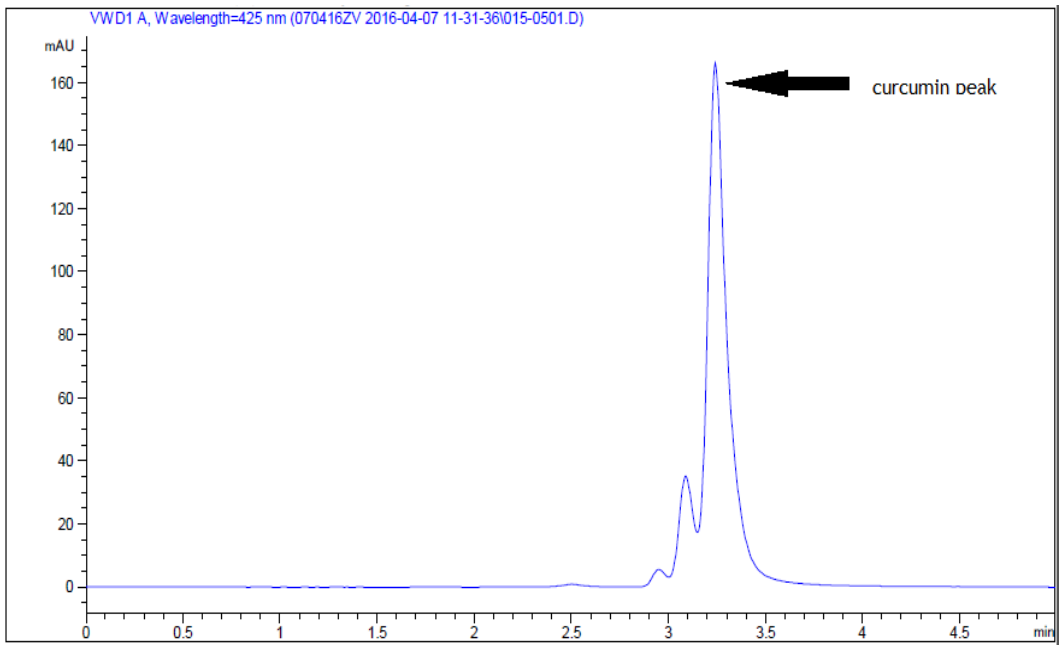

(a)

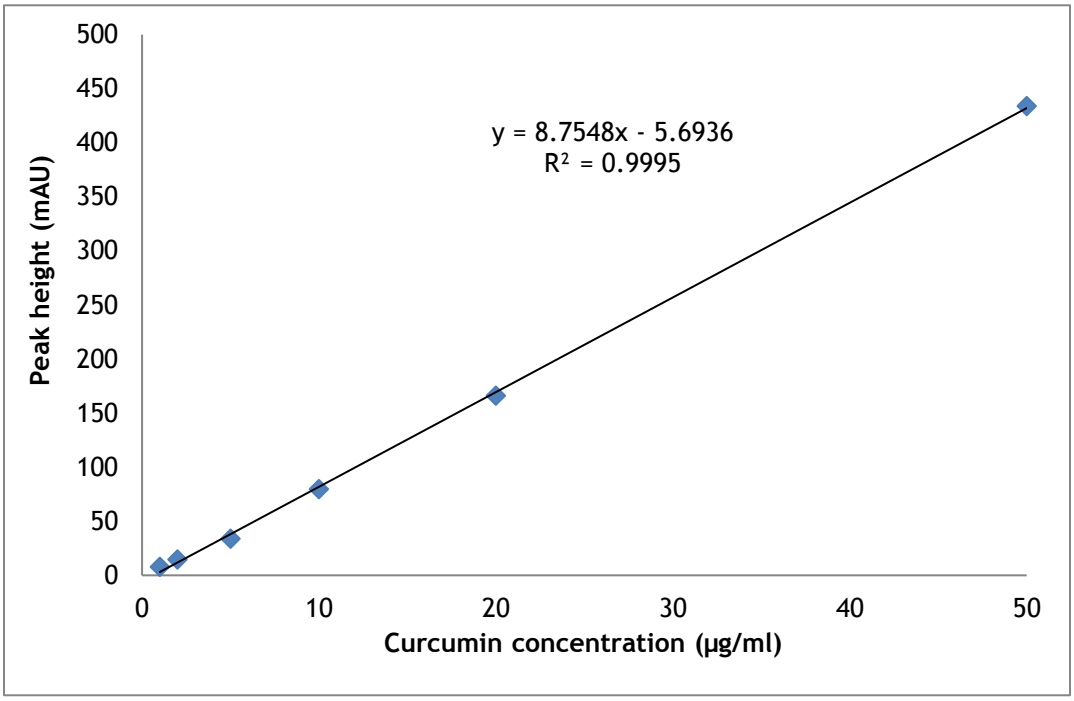

(b)

Fig.2.10. (a) Chromatogram of a curcumin standard (50µg/ml) and (b) Calibration curve of curcumin standards

The small peaks adjacent to the main curcumin peak belong to demethoxycurcumin and bisdemethoxycurcumin. The curcumin standard used in this investigation was 98% in content. Considering the very low concentration (0.1mg/ml) of curcumin that was used as a dye for the experiments, the contribution of the other curcuminoids can be considered negligible.

As discussed before, an increase in 'free curcumin' in solution from a control (no diol) sample to that in an experimental (glucose/fructose) sample will indicate the complexation between boronic acids and diols. Furthermore, the difference in 'free curcumin' levels between the diols would give us an understanding of the affinity of the boronic acids for glucose and fructose. Fig.2.11 portrays the results obtained from this unique investigation. Since it had already been proven that the conjugate with boronic acid to chitosan ratio of 1:1 had the highest adsorption of glucose (from section 2.3.1), this ratio was chosen for further investigation. To further substantiate our hypothesis on the effects of increased crystallinity and/or lack of flexibility of the conjugates at higher boronic acid:chitosan ratios on the sensitivity of the conjugates to glucose adsorption, ratios 2:1 and 3:1 were also chosen for this investigation.

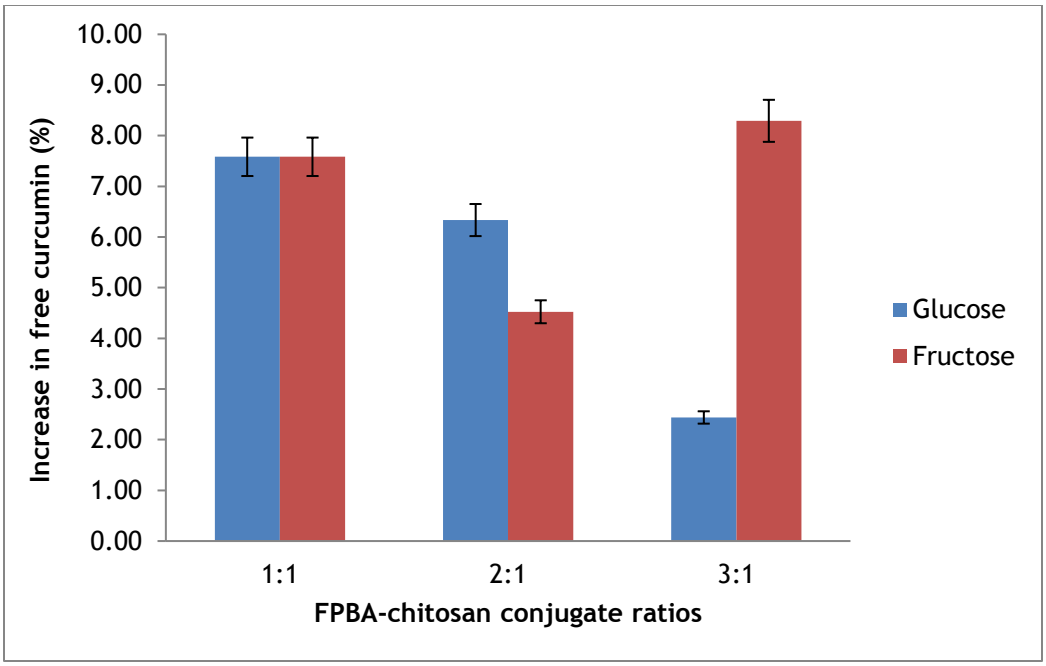

(a)

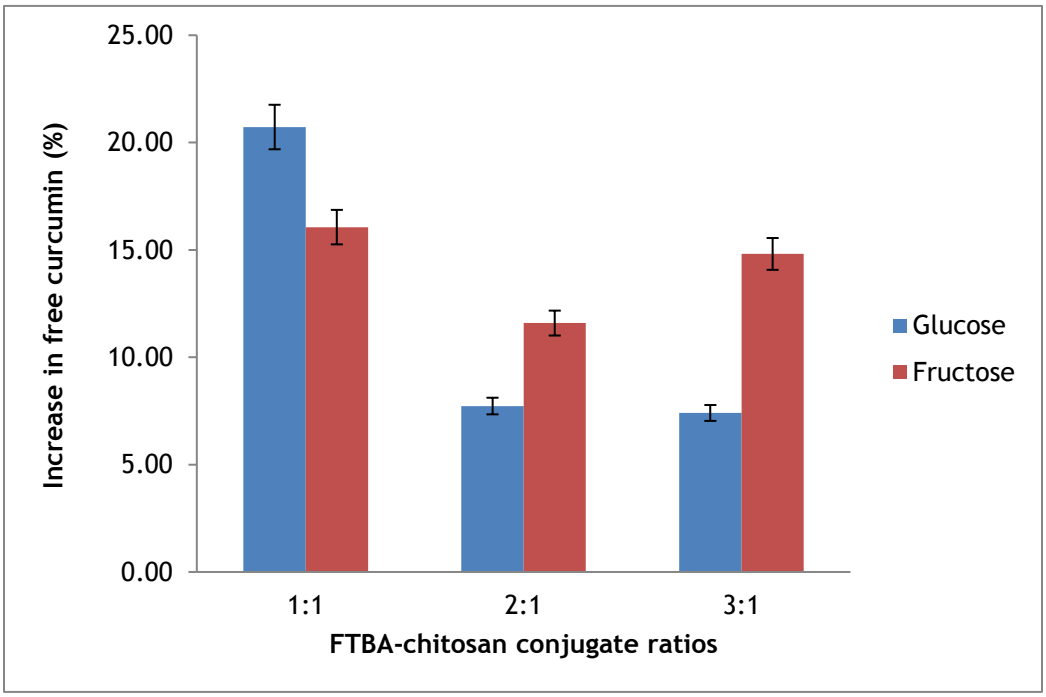

(b)

Fig.2.11. Selectivity of (a) FPBA-chitosan conjugates and (b) FTBA-chitosan conjugates for diols in terms of % increase in 'free curcumin'

It can be seen that, in the presence of glucose, the amount of free curcumin in solution decreases at conjugate ratios above 1:1. This means that at ratios above 1:1, more curcumin is involved in complexing with boronic acids. So, it can be deduced that fewer glucose molecules are occupying the available boronic acid binding moieties at higher ratios; in other words, the affinity of the boronic acid-chitosan conjugates for glucose is decreasing. This observation is in concordance with the previous glucose adsorption data in section 2.3.1 and supplements the proposition that lack of flexibility in the conjugate backbone at higher boronic acid:chitosan ratios might be the principal reason for the decreased affinity of glucose.

Additionally, it should be noted that the % free curcumin in solution at all FTBA ratios is significantly higher than those at respective FPBA ratios ($p<0.025$). Hence, it can be affirmed, once again, that FTBA conjugates have higher affinity than FPBA conjugates for glucose and the notion that the interactions between the thienyl rings (of FTBA), cyclohexane rings (of chitosan backbone) and the hydrocarbon skeleton of glucose is the reason behind the higher propensity of FTBA for glucose appears to be the plausible explanation.

The results with fructose are quite interesting and contrasting to that with glucose. Here, the affinity of both types of the boronic acid conjugates for fructose appears to have decreased from ratio 1:1 to 2:1. SEM studies conducted by Asantewaa et al. proved that at ratios above 1:1, the conjugates become less porous and more crystalline with flat surfaces [50]. Consequently, with increase in crystallinity, the surface area:volume ratio decreases and hence there is less interaction between fructose and boronic acids. However, the affinity of boronic acid conjugates for fructose rises again at 3:1 which is a contradiction to the

theory put forward in the previous sentence. This takes us back to the topic of monovalent interactions of fructose with boronic acid (section 2.1). Wu et al. identified that fructose acts as a monovalent ligand (fig.2.12) in almost all sensing studies performed with boronic acids [48].

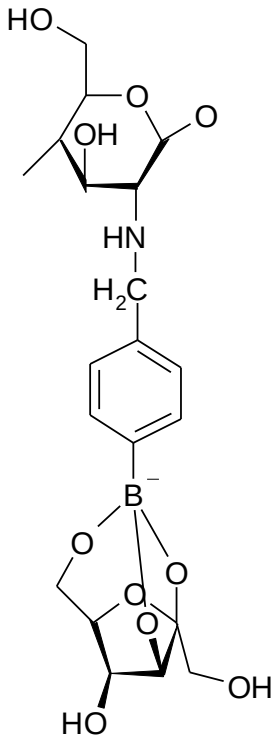

Fig.2.12. Monovalent binding between ß-fructofuranose and boronic acid-chitosan conjugate

Unlike glucose, which has two diol groups involved in multivalent binding with two boronic acid moieties and thus requiring a flexible polymer backbone, fructose appears to overcome the challenge of increased crystallinity with its monovalent interactive option. One molecule of fructose can bind with one boronic acid moiety, so at higher conjugate ratios where the number of boronic acids attached to chitosan is higher, more fructose molecules come together and attach to boronic acids side by side.

One final observation that should be made from fig.2.11 is that, at ratio 1:1, the selectivity (or affinity) of FPBA conjugates for both the diols is the same; for FTBA, the selectivity for glucose is slightly higher (not significant, $p>0.025$). It can be posited that this is the optimum ratio where the conjugates have the ideal number of boronic acids for effective multivalent interactions with glucose. The sum of the strength of these multivalent interactions is at least equal to that of the monovalent interactions between fructose and boronic acids. However, we should also note that both the glucose and fructose concentrations in this investigation were kept the same (2mg/ml). While this is a realistic glucose concentration in biological settings, the fructose concentration in the human blood is at least one thousandth less [54,55]. Considering the fact that the purpose of this project is to develop a GRID for diabetic patients, it can be suggested that both types of boronic acid-chitosan conjugates, designed in the present study, are glucose selective at the concentrations studied and likely to be so in physiological conditions.

2.4. Conclusions

Two different types of boronic acid-chitosan conjugates have been successfully prepared and characterised for their glucose sensitivity. Both FPBA- and FTBA-chitosan conjugates are sensitive to glucose in biologically relevant settings, with FTBA possessing slightly higher affinity for glucose. FPBA/FTBA-chitosan ratio of 1:1 has proved to possess the highest glucose selectivity and will be used to conduct insulin nanoparticle formulation and release studies (chapter 3).

CHAPTER 3

INSULIN LOADED BORONIC ACID SENSOR-BASED CHITOSAN NANOPARTICLES

3.1. Introduction

Biocompatible and biodegradable polymers have attracted much attention by formulation scientists in recent years. Advancements in polymer science and nanotechnology have made it possible for these polymers to be suitably modified with biological and chemical entities for stimuli responsive and targeted drug delivery [56-58]. Chitosan is one such polymer which is synthesized through the deacetylation of chitin (a natural cellulose derivative commonly present in crustaceans such as a crabs and shrimps) in alkaline media. It is mucoadhesive, biocompatible and promotes the passage of biomolecules across biological epithelia [59].

The process of complexing the cationic primary amine groups of chitosan with anionic molecules to prepare controlled-release drug formulations has gained significant attention in the recent past because of the simplicity of the method. Tripolyphosphate (TPP) is the most widely studied polyanion because it is nontoxic, can gel quickly, and electrostatically interacts with positively charged chitosan. Chitosan-TPP nanoparticles (CSNP) possess several desirable physicochemical properties for the delivery of macromolecules and hence have proven to be quite attractive in the pharmaceutical industry [60]. Various researchers have successfully introduced stimuli-responsive moieties such as

concavalin A, glucose oxidase and boronic acids to chitosan with the aim to regulate the release of insulin from their delivery systems [61-63]. This pursuit fits well with the quest for appropriate management of Type 1 diabetes, which necessitates repeated and life-long subcutaneous injections of insulin. In this regard, the formulation of a suitable prototype is aimed at reducing the dosing frequency of subcutaneous injections as the current option.

Presently, our aim is to formulate boronic acid-functionalised chitosan conjugates into a nanoparticulate GRID system. Various approaches have been proposed to encapsulate peptide and protein molecules including ionotropic gelation, polyelectrolyte complexation and layer-by-layer adsorption [64-66]. In our current investigation, two nanoparticulate insulin delivery systems have been prepared via ionotropic gelation with special attention paid to the physicochemical properties, encapsulation efficiency and insulin release of the delivery systems in response to two main physiological diols (glucose and fructose).

3.2. Materials and methods

3.2.1. Materials

Low molecular weight chitosan, sodium tripolyphosphate (TPP), 4-formylphenylboronic acid, 2-formyl-3-thienylboronic acid and sodium borohydride were purchased from Sigma Aldrich (St. Louis, MO, USA); acetic acid, methanol, acetonitrile, fructose and glucose from Thermo Fischer Scientific (Bridgewater, NJ, USA); human recombinant zinc insulin from *P. pastoris* (28.5 IU/mg) was purchased from Merck (Whitehouse, NJ, USA). All other chemicals were of reagent grade.

3.2.2. Investigation of conditions for the formation of CSNP

The nanoparticles were prepared via ionic gelation according to the method adopted by Calvo et al [67]. A stock solution of chitosan (1.5mg/ml) was prepared in 1% acetic acid, and a stock solution of TPP (0.5mg/ml) using milli-Q water. A fixed volume of TPP was then added dropwise to different volumes of chitosan solutions to give various chitosan:TPP ratios (3:1, 4:1, 5:1, 6:1 and 7:1) under constant stirring at 500rpm in room temperature. The mixtures were stirred at the same speed for a further 20 minutes after all the TPP was added. The nanoparticles were prepared in three different pH values (2.9, 4.2 and 5.5) to determine the optimum pH for further studies.

3.2.3. Formulation of insulin loaded boronic acid-functionalised chitosan-TPP nanoparticles

The two different boronic acid- (FPBA and FTBA) chitosan conjugates (chitosan:boronic acid = 1:1) were dissolved in 1% acetic acid to a concentration of 1.5mg/ml and the pH adjusted to 4.2 using 1M NaOH. Insulin (dissolved in 0.01N HCl) was mixed with TPP (0.5mg/ml) to give a final concentration of 0.3mg/ml. The insulin-TPP solution was then added dropwise to the conjugate solutions under magnetic stirring to prepare the two nanoparticulate formulations – FPBAINP and FTBAINP – as described in the previous section. Control nanoparticle formulations were also prepared that did not contain any insulin and were labelled FPBANP and FTBANP.

3.2.4. Physicochemical characterisation of nanoparticles

The size (z-average), polydispersity index (pdi) and charge (zeta potential) of the nanoparticles were assessed using a Zetasizer Nano ZS (Malvern, UK) equipped with a 4Mw He-Ne laser (633 nm). Each analysis was carried out at 25ºC, performed in triplicate and the data expressed as mean ± standard deviation. The morphology and surface topography of nanoparticles were performed by a field emission scanning electron microscope (FESEM, Quanta 400F, FEI Company, USA) under low vacuum and at a viewing voltage of 20.0 kV. After a 1:10 dilution with deionized water, a drop of freshly prepared nanoparticulate solution was placed onto an SEM imaging stub and left to air-dry at room temperature for 24 hours before viewing.

3.2.5. HPLC analysis for insulin content

The amount of insulin in the samples was detected using an Agilent HPLC system equipped with a UV detector. The HPLC parameters are as follows:

- mobile phase - 0.1% aqueous TFA (A) and 0.1% TFA in acetonitrile (B)
- gradient elution with the mobile phase starting with 75% of A and decreasing to 40% over 7 min
- flow rate – 1 ml/min
- injection volume – 20µl
- detection wavelength – 214 nm
- column – Agilent Zorbax 300SB-4.6 x 250 mm C_{18}, with particle size of 5 µm and pore size of 300 Å.

The calibration curve was constructed from pure insulin dissolved in 0.01N HCl at a range of 1 - 100µg/ml.

3.2.6. Evaluation of encapsulation efficiencies of nanoparticles

The encapsulation efficiency (EE%) of insulin within the nanoparticles was determined upon separation of the nanoparticles from the aqueous media containing free insulin by centrifugation at 14000 rpm for 20 min using a Beckman Coulter Microfuge 16 centrifuge (Beckman Coulter, USA). The amount of free insulin in the supernatant was measured using the above HPLC procedure by comparing peak area obtained with that from the calibration curve. The EE% for insulin was calculated as:

$$\text{EE\%} = \frac{\text{total insulin in formulation} - \text{free insulin in supernatant}}{\text{total insulin in formulation}} \times 100\%$$

3.2.7. In vitro insulin release studies

The amount of insulin released from the nanoparticles was studied in six different media – deionised water, glucose (1, 2 and 3mg/ml), fructose (0.002mg/ml) and glucose (2mg/ml)+fructose (0.002mg/ml). Several 100 µl replicas of FPBAINP and FTBAINP were placed in Eppendorf tubes containing 1 ml of the various release media and incubated at 37ºC with horizontal shaking at 100 rpm on a WiseCube WIS-20, Precise Shaking Incubator. At predetermined time points, one of the seeded tubes was withdrawn and centrifuged at 14000 rpm for 5 minutes using a Beckman Coulter Microfuge 16 centrifuge which was followed by injection of 20 µl of the supernatant into the HPLC system. The amount of insulin released in the respective media was computed by comparing peak area obtained with those from the calibration curve.

3.3. Results and Discussion

3.3.1. Optimisation of conditions for CSNP preparation

The size of colloidal systems is an important parameter that determines the systems' ability to deliver drugs to the target site effectively. Particles larger than 1μm are too large to diffuse through the blood-brain barrier and hence remain at the site of injection. Smaller particles have a better propensity for diffusing across tissue and this property has found wide appeal to cancer researchers who aim to target cancerous cells with drug-loaded nanoparticles. Ideally, a particle size of 100 – 300nm is desirable for *in vitro* and *in vivo* studies [60]. Fig.3.1 shows the changes in the size of the CSNP of various chitosan:TPP ratios and in the three different pH conditions.

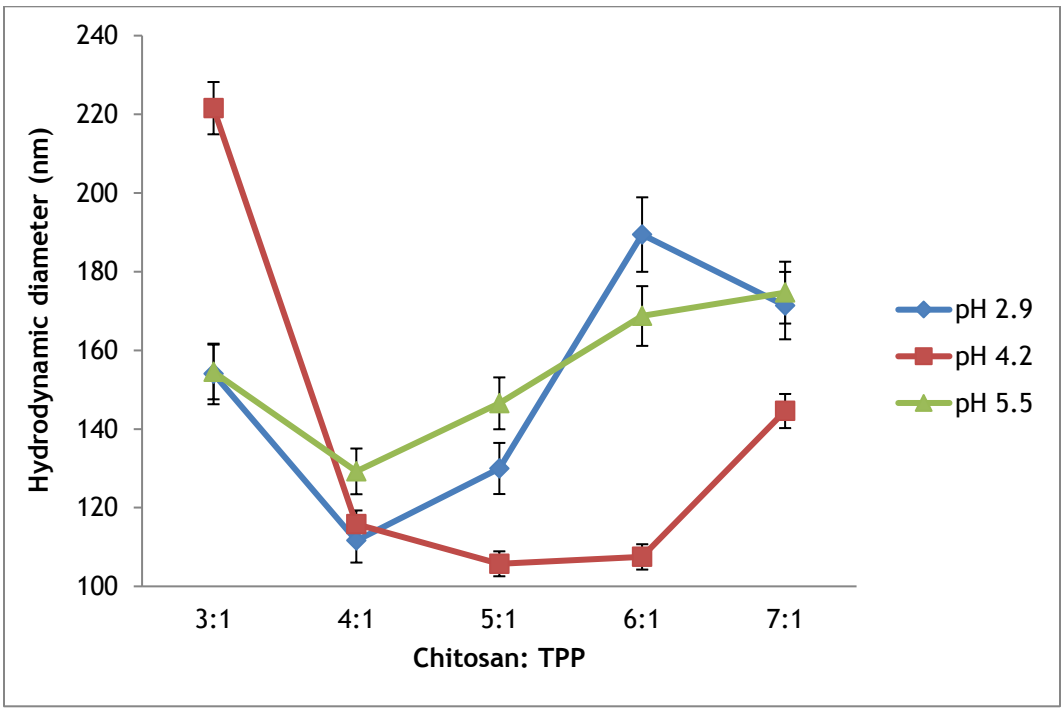

Fig.3.1. Mean particle size of the nanoparticles as a function of chitosan-TPP ratios in different pH conditions.

In all three pH, the size of the nanoparticles drops sharply from ratio 3:1 to 4:1 before rising again at higher ratios. CSNP are formed by the crosslinking of positively charged chitosan chains with the negatively charged TPP ions. Chitosan chains become positively charged due to the protonation of their primary amine groups in acidic media (NH_3^+), however, not all the amine groups protonate in solution. The overall degree of protonation increases as the amount of chitosan increases.

At 3:1 ratio, it can be hypothesised that there were not enough cationic moieties within the chitosan polymer chains to manifest an overall positive charge on the nanoparticles. This relatively lower surface charge on the particles promotes attractive van der Waals forces between the particles as opposed to repulsion at higher surface charges. This consequently causes the particles to aggregate and hence register higher z-average readings. A ratio of chitosan to TPP of 4:1 appears to be optimum for the retention of sufficient positively charged chitosan moieties (NH_3^+) to effectively complex with the anionic TPP ions ($P_3O_{10}^-$) resulting in the quenching of the anionic charge contribution and formation of a strongly positive residually charged nanoparticles. As the nanoparticles have an overall strong positive charge, they repel each other and do not aggregate as in ratio 3:1. At ratios higher than 5:1, it can be postulated that the amount of TPP is insufficient to provide requisite anionic charge density to effectively crosslink the chitosan chains and form stable nanocomplexes. This ultimately causes the nanoparticles to have the tendency to form aggregates.

The size of the nanoparticles appears to vary according to the pH environment as well. In general, the particle size increases as the pH increases. At lower pH, there is effective crosslinking between the chitosan chains by the TPP to form

stable nanoparticles because there are very little OH^- ions available in the medium. However, as the pH of the media is increased, more OH^- ions are available in solution. Since OH^- ions are much smaller than TPP ions, they can penetrate the chitosan gel matrix a lot more easily and hence compete with the TPP ions for interaction with the positively charged chitosan. Consequently, the nanoparticle matrix destabilises at higher pH resulting in an increase in the overall size of the particles. Mattu et al. [68] also obtained similar results in the size of their chitosan nanoparticles with an increase in pH of the medium and attributed this observation to the presence of increased OH^- ions in solution.

3.3.2. Preparation of insulin loaded nanoparticles

After careful analysis of all the physicochemical parameters, and from a stability standpoint, chitosan:TPP ratio of 4:1 and a pH of 4.2 were chosen to be the optimum conditions for the preparation of insulin containing nanoparticles. Table 3.1 shows the size, charge and pdi of the various nanoparticle formulations.

Formulae	Diameter (nm)	Zeta potential (mV)	Pdi
CSNP	111.6 ± 2.3	59.0 ± 11.3	0.26
FPBANP	147.4 ± 13.7	30.8 ± 7.9	0.32
FPBAINP	170.1 ± 14.2	23.4 ± 4.5	0.31
FTBANP	138.5 ± 5.9	27.9 ± 4.3	0.19
FTBAINP	162.7 ± 9.8	22.2 ± 2.5	0.22

Data shown are the mean ± standard deviation (n = 3).

Table 3.1. Physicochemical parameters of the nanoparticulate formulations

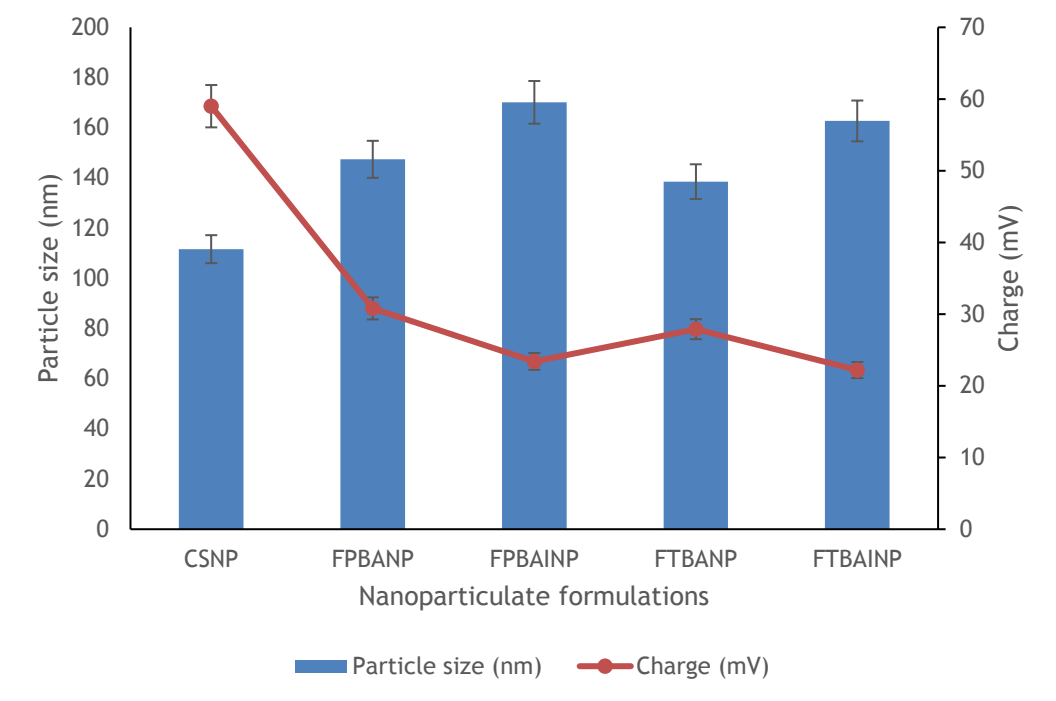

Fig. 3.2. Physicochemical characteristics of the nanoparticulate formulations

The general trend in size follows the order of BAINP > BANP > CSNP. Indeed the boronic acid chitosan conjugates are larger in structure than the native chitosan and hence results in the formation of larger insulin-free nanoparticles. The consumption of the amine groups of chitosan during the reductive N-alkylation to form the conjugates means that chitosan is less positively charged and hence the overall charge of the nanoparticles is lower. Insulin loaded nanoparticles are the largest because of the introduction of insulin molecule into the nanoparticulate matrix. The negative charge of insulin contributes to a slight reduction in the total charge of the nanoparticles as well.

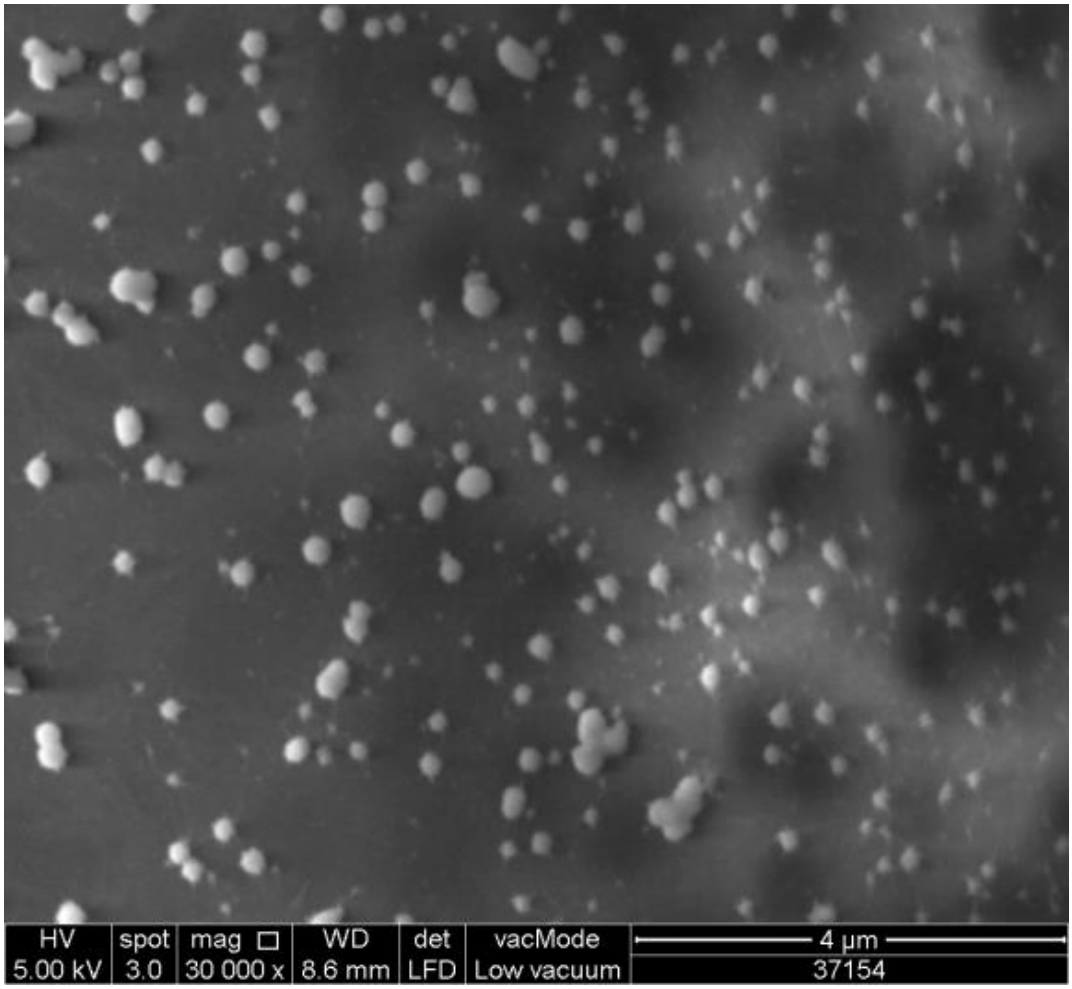
HV
5.00 kV
spot
3.0
mag
30 000 x
WD
8.6 mm
det
LFD
vacMode
Low vacuum
4 µm
37154

(a)

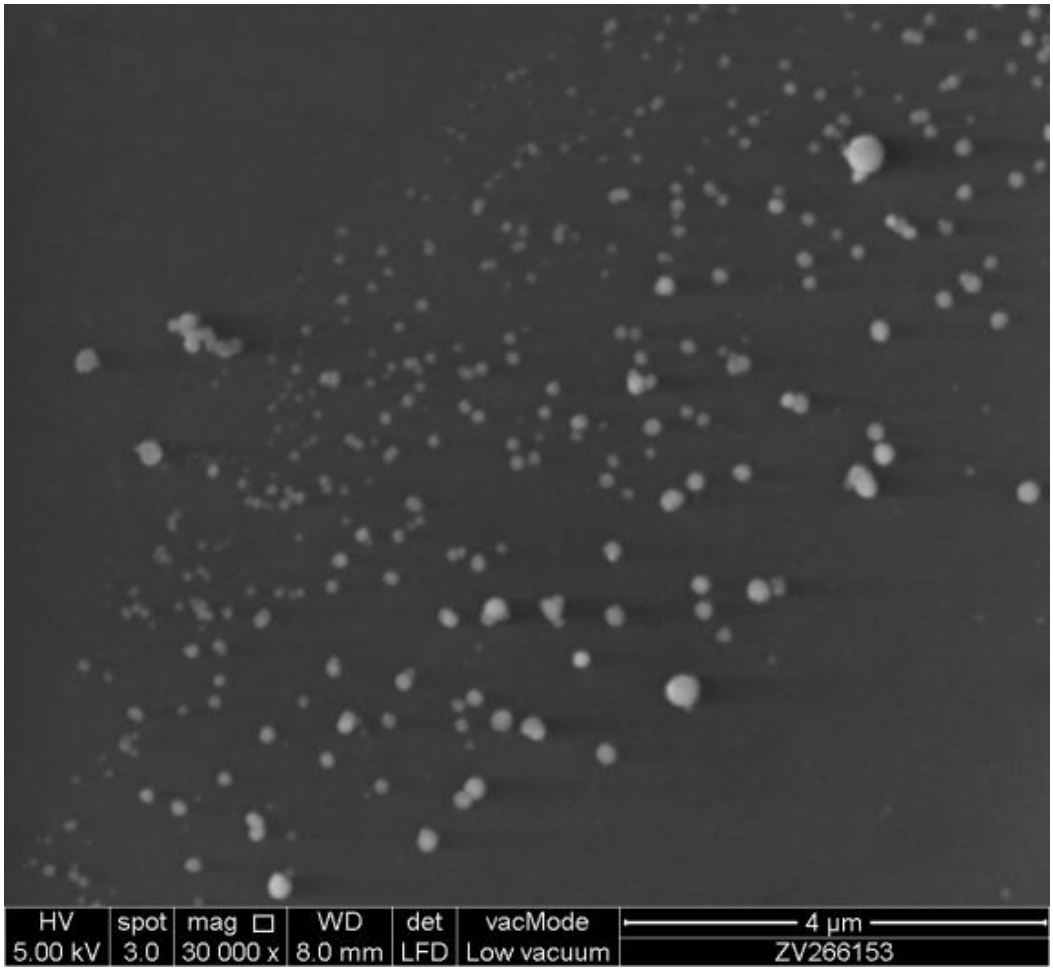

(b)

Fig.3.3. Scanning electron microphotography of (a) FPBAINP and (b) FTBAINP

Overall, the average diameters of the target nanoparticles – FPBAINP and FTBAINP – are reasonably small and the formulations are homogenous (as indicated by the pdi value). Nanoparticles with a surface charge of |10| mV are considered approximately neutral; while nanoparticles with zeta potentials of at least |30| mV are considered strongly ionic, thereby ensuring sufficient repulsive forces to keep the particles apart [69]. In that respect, the overall charges of the formulations are slightly on the lower side. Notwithstanding, FPBAINP and

FTBAINP appear to be reasonably separated from each other as shown in the FESEM images in fig.3.2. The particles also appear spherical and in agreement with the z-average determinations.

3.3.3. Percentage encapsulation efficiency (EE%)

The drug release profile and pharmaceutical cost-effectiveness of a formulation depend on the drug loading capacity or the encapsulation efficiency (EE %) within the carrier system. This is particularly crucial for nanoparticulate delivery systems which have the smallest surface area-to-volume ratio of all dosage forms. The EE% for FPBAINP and FTBAINP were 56.7% and 57.5% respectively. Fig.3.3a and b show the chromatograph obtained from the HPLC analysis of an insulin standard and the calibration curve of the standards respectively. There is a range of reported EE% of insulin in nanoparticulate drug delivery systems. Zhang et al. [70] reported an insulin loading capacity of more than 78% in their polyethylene grafted chitosan nanoparticles, whilst Zhu et al. [71] prepared PEG modified N-trimethylaminoethylmethacrylate chitosan nanoparticles which resulted in a range of EE% from 10 – 84% depending on the initial weight of the polymer used in the formulation. Wu et al. [63] formulated nanoparticles with an EE% ranging from 49 – 59% and contend that this variability was attributed to the amount of insulin used and the molecular weight of the polymer.

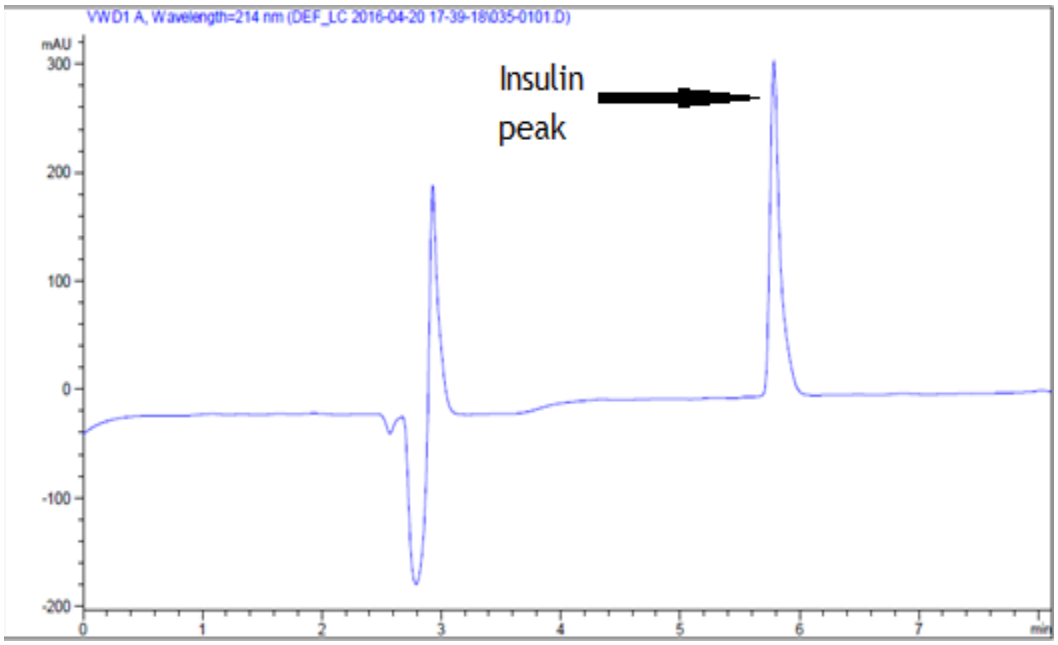

(a)

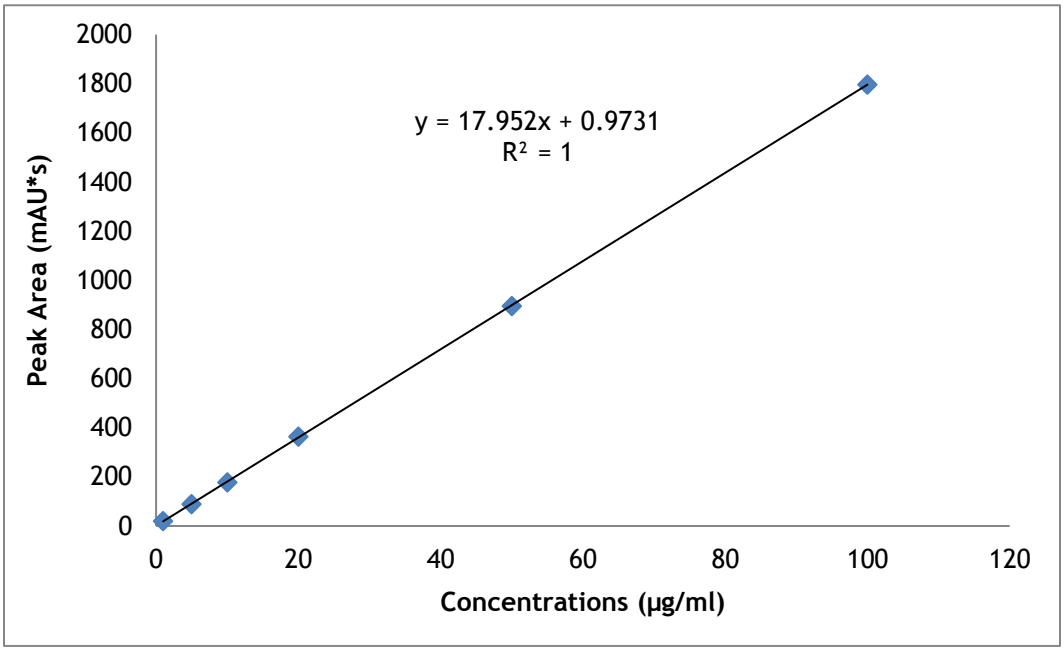

(b)

Fig.3.4. (a) Chromatogram of insulin standard (100µg/ml) and (b) Calibration curve of insulin standards

We may conclude that the EE% obtained in the present investigation is comparable to those reported in the literature. One of the initial hypothesis for choosing FTBA as the glucose sensor was the presence of sulphur in its structure. It was assumed that sulphur would lead to a higher encapsulation of insulin into the nanoparticulate matrix via additional interactions with the disulphide bridges present in the structure of insulin. However, the EE% of FPBAINP, which lacks the sulphur atom, is comparable to that of FTBAINP which might imply that the sulphur (in FTBA) has little or no effect in additional insulin encapsulation in the present scenario.

3.3.4. In vitro insulin release in various media

The primary objective of this project is to formulate an insulin delivery system that is glucose sensitive. In chapter 2, we have proven the superior selectivity of FPBA- and FTBA-chitosan conjugates (at BA:chitosan ratio of 1:1) for glucose compared to fructose by discussing the chemistry of the conjugates in the presence of the diols. The current chapter further substantiates the selectivity of the two conjugates for glucose by the physiochemical behaviour of the nanoparticulate formulations of the conjugates. To prove our theory, FPBAINP and FTBAINP were exposed to different media. Three different blood concentrations of glucose were used to test the glucose dependent release of insulin. Deionised water was used to check the leaking of the nanoparticles. A blood concentration (diabetic) of fructose only was used to check how much insulin was released and another media had both glucose and fructose of concentrations similar to that in the blood of a diabetic patient to check the amount of insulin released. Fig.3.4a and b show the insulin release profiles of the two nanoparticle formulations in the six different media used.

In FPBAINP (fig.3.4a), an initial burst phase of insulin release followed by a more sustained release was observed in all media. The burst phase can be attributed to the release of insulin that is entrapped toward the edge of the nanoparticulate matrix. The sustained release is of the insulin that is present within the deeper pockets of the core matrix. However, the amount of insulin released during the burst phase varied depending on the external media.

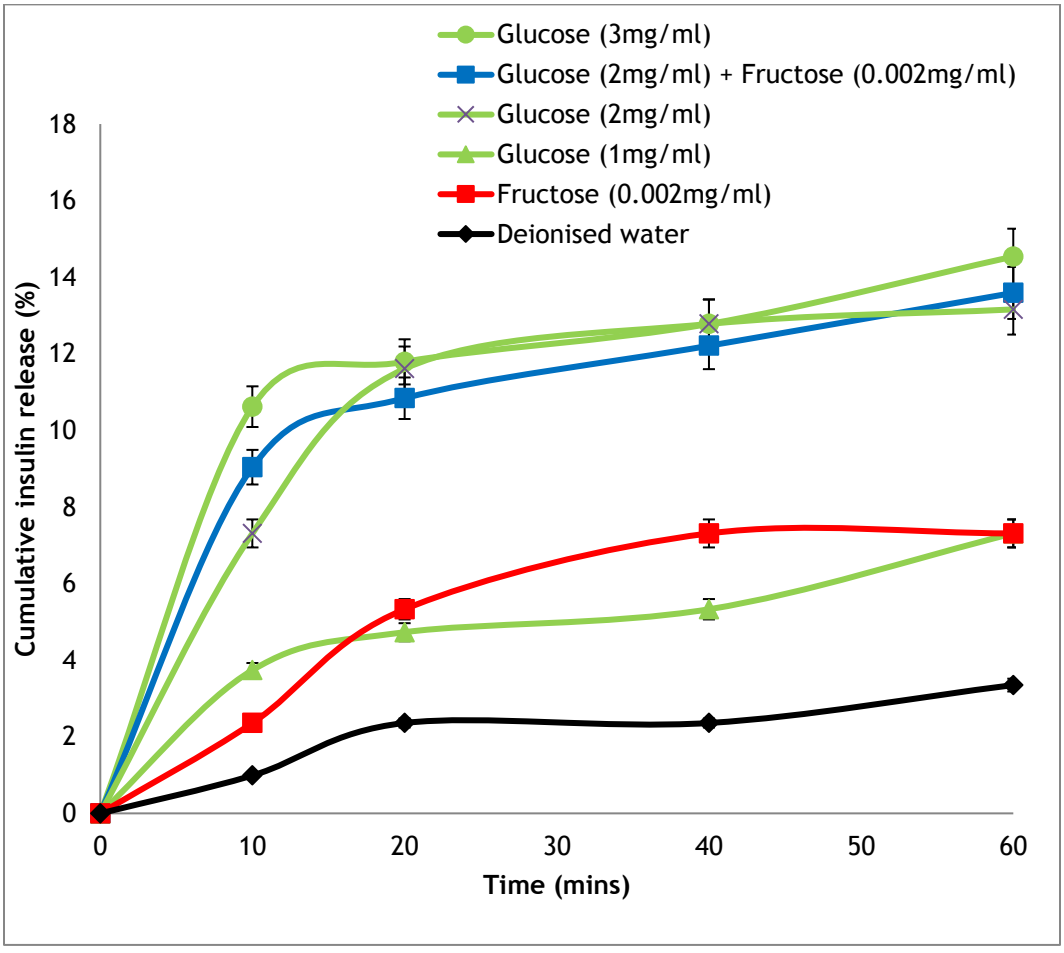

(a)

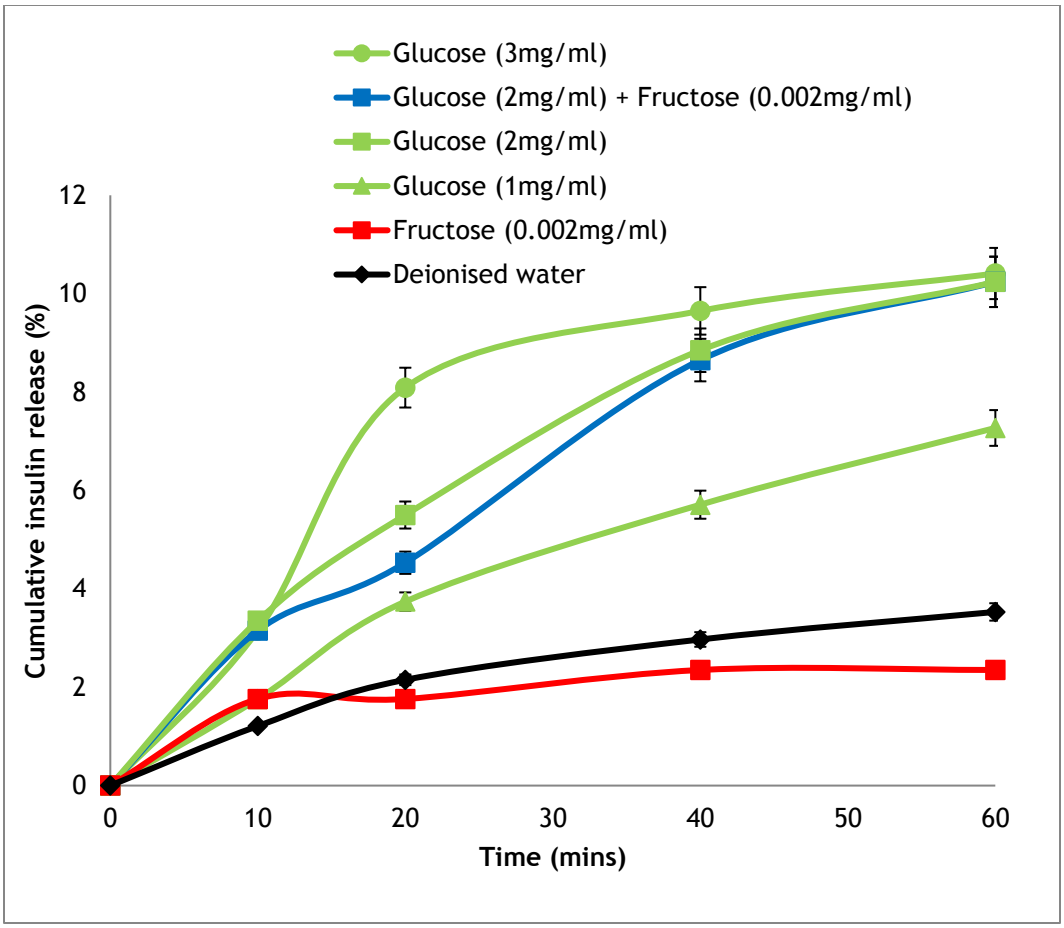

(b)

Fig. 3.5. Insulin release profiles of (a) FPBAINP and (b) FTBAINP in various media

A similar pattern of insulin release was observed in FTBAINP formulation as well. In both FPBAINP and FTBAINP, the amount of insulin released within the first 10-20 minutes increased as the concentration of external glucose media increased from 1 – 3mg/ml. In fact, within the first 20 mins the amount of insulin released from both the formulations in glucose media (3mg/ml) was at least twice that in glucose media (1mg/ml). Springsteen et al. [51] noted that at higher glucose concentrations, the rate of interaction between glucose and boronic acid is higher; hence a faster rate of insulin release occurred in this instance. This

behaviour of our systems proves their glucose concentration dependent insulin release potential.

Not only are the EE% of the two formulations similar, but the total amount of insulin released after one hour is also almost equal in FPBAINP and FTBAINP. Both formulations have minimal leakage as the total amount of insulin released after one hour is below 4%.

Interestingly, the total amount of insulin released from FPBAINP in fructose is higher than that released from FTBAINP in the same media. This observation might be the result of fewer interactions between fructose and FTBA moieties than with FPBA moieties and hence allude to the fact that FTBA has lower affinity for fructose than FPBA. This implication will be of significant advantage in developing a GRID; however, it is imperative to conduct further investigations before any assertion is made.

It should also be noted that the amount of insulin released from both the formulations in fructose (of blood concentration) is similar to that released in deionised water and/or glucose (1mg/ml). Furthermore, in glucose+fructose media, the total amount of insulin released from both the systems is similar to that released in 2mg/ml glucose media. Considering the fact that both media had the same concentration of glucose and the only difference was the (blood concentration) of fructose, it can be contended that both FPBAINP and FTBAINP are glucose selective in physiological settings. The presence of minute amounts of fructose (which is similar to that in human blood) does not appear to have a marked effect in insulin release from the two systems. These observations further validate the theory discussed in chapter 2 about the stronger multivalent

bindings between the boronic acid conjugated chitosan with glucose than the monovalent interactions with fructose and hence confirm the higher selectivity of the conjugates for glucose than for fructose in biological conditions.

3.4. Conclusions

Two different boronic acid conjugated chitosans have been formulated into insulin loaded nanoparticles. The formulations were then investigated for their physicochemical properties and insulin release in various media. The nanoparticles in both the formulations were small, reasonably charged and homogenous promising good stability. The EE% of insulin of both FPBAINP and FTBAINP were similar and comparable to those published in the literature. Both the systems released insulin predominantly in the presence of glucose and show great potential to be successful GRIDs.

FUTURE WORK

In this project, a chitosan-based nanoparticulate GRID system has been developed and its potential has been studied via various investigations. However, for approval of clinical trials, further experiments need to be carried out and some of these include the following:

- Preparation of a larger set of boronic acid-chitosan conjugate ratios and characterisation of their selectivity for diols as a function of the degree of boronic acid conjugation to chitosan
- Formulation of insulin-loaded chitosan nanoparticles at physiological pH
- Cytotoxicity and biocompatibility studies of the nanoparticles
- Stability studies of the nanoparticles
- *In vitro* insulin release studies for a longer period of time to determine the lifetime of the formulated GRID system
- *In vivo* studies to investigate the potential of the GRID

References

1. American Diabetes Association. Standards of medical care in diabetes – 2013. *Diabetes Care* **2014**, *37*, S14–S80.
2. Shaw, J.; Sicree, R.; Zimmet, P. Global estimates of the prevalence of diabetes for 2010 and 2030. *Diabetes Res. Clin. Pract.* **2010**, *87*, 4–14.
3. Zhang P.; Zhang X.; Brown J.; Vistisen D.; Sicree R.; Shaw J.; Nichols G. Global healthcare expenditure on diabetes for 2010 and 2030. *Diabetes Res. Clin. Pract.* **2010**, *87*, 293–301.
4. Lieberman, S.; DiLorenzo, T. Comprehensive guide to antibody and T-cell responses in type 1 diabetes. *Tissue Antigens* **2003**, *62*, 359–377.
5. Donath, M.; Shoelson, S. Type 2 diabetes as an inflammatory disease. *Nature Rev. Immunol.* **2011**, *11*, 98–107.
6. Dabelea, D. The accelerating epidemic of childhood diabetes. *Lancet* **2009**, *373*, 1999–2000.
7. Heinemann, L. New ways of insulin delivery. *Int. J. Clin. Pract.* **2011**, *65*, 31–46.
8. American Diabetes Association. Standards of medical care in diabetes – 2013. *Diabetes Care* **2013**, *36*, 11–66.
9. Sarwar N.; Gao P.; Seshasai S.; Gobin R.; Kaptoge S.; Angelantonio E.; Ingelsson E.; Lawlor D.; Selvin E.; Stampfer M.; Stehouwer C.; Lewington S.; Pennells L.; Thompson A.; Sattar N.; White I.; Ray K.; Danesh J. Diabetes mellitus, fasting blood glucose concentration, and risk of vascular disease: a collaborative meta-analysis of 102 prospective studies. *Lancet* **2010**, *375*, 2215–2222.

10. Schulman R.; Moshier E.; Rho L.; Casey M.; Godbold J.; Mechanick J. Association of glycemic control parameters with clinical outcomes in chronic critical illness. *Endocr. Pract.* **2014**, *20*, 884–893.
11. Berenson, D.; Weiss, A.; Wan, Z.; Weiss, M. Insulin analogs for the treatment of diabetes mellitus: therapeutic applications of protein engineering. *Ann. NY Acad. Sci.* **2011**, *1243*, 40–54.
12. Tamborlane, W. Continuous glucose monitoring and intensive treatment of type 1 diabetes. *N. Engl. J. Med.* **2008**, *359*, 1464–1476.
13. Veiseh, O.; Tang, B.; Whitehead, K.; Anderson, D.; Langer, R. Managing diabetes with nanomedicine: challenges and opportunities. *Nat. Rev. Drug Discov.* **2015**, *14*, 45-57.
14. Pickup, J. Insulin-pump therapy for type 1 diabetes mellitus. *N. Engl. J. Med.* **2012**, *366*, 1616–1624.
15. Owens, D. New horizons – alternative routes for insulin therapy. *Nat. Rev. Drug Discov.* **2002**, *1*, 529–540.
16. Mehanna, A. Antidiabetic agents: past, present and future. *Future Med. Chem.* **2013**, *5*, 411–430.
17. Hovorka, R.; Nodale, M.; Haidar, A.; Wilinska, M. Assessing performance of closed-loop insulin delivery systems by continuous glucose monitoring: drawbacks and way forward. *Diabetes Technol. Ther.* **2013**, *15*, 4–12.
18. Hinchcliffe M.; Illum, L. Intranasal insulin delivery and therapy. *Adv. Drug Deliver. Rev.* **1999**, *35*, 199-234.
19. Chang, S.; Chien, Y. Intranasal drug administration for systemic medication. *Pharm. Int.* **1984**, *5*, 287–288.

20. Lee, V.; Yamamoto, A. Penetration and enzymic barriers to peptide and protein absorption. *Adv. Drug Deliv. Rev.* **1990**, *4*, 171–207.
21. Illum, L. Nasal delivery of peptides, factors affecting nasal absorption, in: D.J.A. Crommelin, K.K. Midha (Eds.), Topics in Pharmaceutical Sciences, Medpharm Scientific, Stuttgart, **1992**, pp. 71–82.
22. Weissleder, R.; Pittet, M. Imaging in the era of molecular oncology. *Nature* **2008**, *452*, 580–589.
23. Whitesides, G. The 'right' size in nanobiotechnology. *Nature Biotech.* **2003**, *21*, 1161–1165.
24. Dvir, T.; Timko, B.; Kohane, D.; Langer, R. Nanotechnological strategies for engineering complex tissues. *Nature Nanotech.* **2011**, *6*, 13–22.
25. Schroeder, A.; Heller, D.; Winslow, M.; Dahlman, J.; Pratt, G.; Langer, R.; Jacks, T.; Anderson, D. Treating metastatic cancer with nanotechnology. *Nature Rev. Cancer* **2012**, *12*, 39–50.
26. Venkatraman, S.; Ma, L.; Natarajan, J.; Chattopadhyay, S. Polymer- and liposome-based nanoparticles in targeted drug delivery. *Front. Biosci.* **2010**, *2*, 801–814.
27. Stinchcombe, T. Nanoparticle albumin-bound paclitaxel: a novel Cremphor-EL-free formulation of paclitaxel. *Nanomed.* **2007**, *2*, 415–423.
28. Barbas, A.; Mi, J.; Clary, B.; White, R. Aptamer applications for targeted cancer therapy. *Future Oncol.* **2010**, *6*, 1117–1126.
29. Chiu, G. Lipid-based nanoparticulate systems for the delivery of anti-cancer drug cocktails: Implications on pharmacokinetics and drug toxicities. *Curr. Drug Metab.* **2009**, *10*, 861–874.

30. Schroeder, A.; Levins, C.; Cortez, C.; Langer, R.; Anderson, D.; Lipid-based nanotherapeutics for siRNA delivery. *J. Intern. Med.* **2010**, *267*, 9–21.
31. Zion, T. Glucose-responsive materials for self-regulated insulin delivery. Thesis, Massachusetts Institute of Technology **2004**.
32. Stuart, M.; Huck, W.; Genzer, J.; Müller, M.; Ober, C.; Stamm, M.; Sukhorukov, G.; Szleifer, I.; Tsukruk, V.; Urban, M.; Winnik, F.; Zauscher, S.; Luzinov, I.; Minko, S. Emerging applications of stimuli-responsive polymer materials. *Nature Mater.* **2010**, *9*, 101–113.
33. Wu, W.; Mitra, N.; Yan, E.; Zhou, S. Multifunctional hybrid nanogel for integration of optical glucose sensing and self-regulated insulin release at physiological pH. *ACS Nano*, **2010**, *4*, 4831–4839.
34. Fischel-Ghodsian, F.; Brown, L.; Mathiowitz, E.; Brandenburg, D.; Langer, R. Enzymatically controlled drug delivery. *Proc. Natl Acad. Sci. USA* **1988**, *85*, 2403–2406.
35. Gu, Z.; Tram T.; Dang, S.; Ma, M. Glucose-responsive microgels integrated with enzyme nanocapsules for closed-loop insulin delivery. *ACS Nano* **2013**, *7*, 6758–6766.
36. Qi, W.; Yan, X.; Fei, J.; Wang, A.; Cui, Y.; Li, J. Triggered release of insulin from glucose-sensitive enzyme multilayer shells. *Biomaterials* **2009**, *30*, 2799–2806.
37. Luo, J.; Cao, S.; Chen, X.; Liu, S.; Tan, H.; Wu, W.; Li, J. Super long-term glycemic control in diabetic rats by glucose-sensitive LbL films constructed of supramolecular insulin assembly. *Biomaterials* **2012**, *33*, 8733–8742.

38. Brownlee, M.; Cerami, A. A glucose-controlled insulin-delivery system: semisynthetic insulin bound to lectin. *Science* **1979**, *206*, 1190–1191.
39. Powell, A.; Leon, M. Reversible interaction of human lymphocytes with the mitogen concanavalin A. *Exp. Cell Res.* **1970**, *62*, 315–325.
40. Fonte, P.; Araújo, F.; Silva, C.; Pereira, C.; Reis, S.; Santos, H.; Sarmento, B. Polymer-based nanoparticles for oral insulin delivery: Revisited approaches. *Biotechnol. Adv.* **2015**, *33*, 1342-1354.
41. Xiong, X.; Li, Y.; Li, Z.; Zhou, C.; Tam, K.; Liu, Z. Vesicles from pluronic/poly(lactic acid) block copolymers as new carriers for oral insulin delivery. *J. Control. Release* **2007**, *120*, 11–7.
42. Xiong, Y.; Li, Q.; Li, Y.; Guo, L.; Li, Z.; Gong, Y. Pluronic P85/poly(lactic acid) vesicles as novel carrier for oral insulin delivery. *Colloids Surf. B. Biointerfaces* **2013**, *111*, 282–8.
43. Yang, J.; Sun, H.; Song, C. Preparation, characterization and in vivo evaluation of pH-sensitive oral insulin-loaded poly(lactic-co-glycolicacid) nanoparticles. *Diabetes Obes. Metab.* **2012**, *14*, 358–64.
44. Chalasani, B.; Russell-Jones, G.; Jain, A.; Diwan, P.; Jain, S. Effective oral delivery of insulin in animal models using vitamin B12-coated dextran nanoparticles. *J. Control. Release* **2007**, *122*, 141–50.
45. Makhlof, A.; Tozuka, Y.; Takeuchi, H. Design and evaluation of novel pH-sensitive chitosan nanoparticles for oral insulin delivery. *Eur. J. Pharm. Sci.* **2011**, *42*, 445–51.
46. Sonaje, K.; Chuang, E.; Lin, K.; Yen, T.; Su, F.; Tseng, M. Opening of epithelial tight junctions and enhancement of paracellular permeation by

chitosan: microscopic, ultrastructural, and computed-tomographic observations. *Mol. Pharm.* **2012**, *9*, 1271–9.

47. Pan, Y.; Li, Y.; Zhao, H.; Zheng, J.; Xu, H.; Wei, G. Bioadhesive polysaccharide in protein delivery system: chitosan nanoparticles improve the intestinal absorption of insulin in vivo. *Int. J. Pharm.* **2002**, *249*, 139–47.
48. Wu, X.; Li, Z.; Chen, X.; Fossey, J.; James, T.; Jiang, Y. Selective sensing of saccharides using simple boronic acids and their aggregates. *Chem. Soc. Rev.* **2013**, *42*, 8032-8048.
49. Lorand, J.; Edwards, J. Polyol Complexes and Structure of the Benzeneboronate Ion. *J. Org. Chem.* **1959**, *24*, 769–774.
50. Asantewaa, Y.; Aylott, J.; Burley, J.; Billa, N.; Roberts, C. Correlating physicochemical properties of boronic acid – chitosan conjugates to glucose adsorption sensitivity. *Pharmaceutics* **2013**, *5*, 69-80.
51. Springsteen, G.; Wang, B. A detailed examination of boronic acid–diol complexation. *Tetrahedron* **2002**, *58*, 5291–5300.
52. Lawrence, K.; Flower, S.; Kociok-Kohn, G.; Frost, C.; James, T. A simple and effective colorimetric technique for the detection of boronic acids and their derivatives. *Anal. Methods* **2012**, *4*, 2215-2217.
53. Kittur, F.; Harigh, P.; Udaya, S.; Tharanathan, R. Synthesis and characterization of a novel derivative of chitosan. *Carbohydr. Polym.* **2002**, *49*, 185–193.
54. Yao, Y.; Zhao, L.; Yang, J. Glucose–responsive vehicles containing phenylborate ester for controlled insulin release at neutral pH. *Biomacromolecules* **2012**, *13*, 1837–44.

55. Kawasaki, T.; Akanuma, H.; Yamanouchi, T. Increased fructose concentrations in blood and urine in patients with diabetes. *Diabetes Care* **2002**, *25*, 353–357.

56. Xu, J.; Gao, F.; Li, L.; Ma, H.; Fan, Y.; Liu, W.; Guo,S.; Zhao, X.; Wang, H. Gelatin–mesoporous silica nanoparticles as matrix metalloproteinases-degradable drug delivery systems in vivo. *Micropor. Mesopor. Mat.* **2013**, *182*, 165–172.

57. Rao, L.; Bu, L.; Xu, J.; Cai, B.; Yu, G.; Yu, X.; He, Z.; Huang, Q.; Li, A.; Guo, S.; Zhang, W.; Liu, W.; Sun, Z.; Wang, H.; Wang, T.; Zhao, X. Red Blood Cell Membrane as a Biomimetic Nanocoating for Prolonged Circulation Time and Reduced Accelerated Blood Clearance. *Small* **2015**, *11*, 6225–6236.

58. Rao, L.; Bu, L.; Xu, J.; Cai, B.; Li, A.; Zhang, W.; Sun, Z.; Guo, S.; Liu, W.; Wang, T.; Zhao, X. Cancer Cell Membrane-Coated Upconversion Nanoprobes for Highly Specific Tumor Imaging. *Adv. Mater.* **2016**, *28*, 3460–3466.

59. Kean, T.; Thanou, M. Biodegradation, biodistribution and toxicity of chitosan. *Adv. Drug Deliver. Rev.* **2010**, *62*, 3–11.

60. Yang, H.; Hon, M. The effect of the molecular weight of chitosan nanoparticles and its application on drug delivery. *Microchem. J.* **2009**, *92*, 87-91.

61. Wu, H.; Wang, J.; Kang, X.; Wang, C.; Wang, D.; Liu, J.; Aksay, I.; Lin, Y. Glucose biosensor based on immobilization of glucose oxidase in platinum nanoparticles/graphene/chitosan nanocomposite film. *Talanta* **2009**, *80*, 403–6.

62. Yin, L.; Ding, J.; He, C.; Cui, L.; Tang, C.; Yin, C. Drug permeability and mucoadhesion properties of thiolated trimethyl chitosan nanoparticles in oral insulin delivery. *Biomaterials* **2009**, *30*, 5691-700.
63. Wu, Z.; Zhang, S.; Zhang, X.; Shu, S.; Chu, T.; Yu, D. Phenylboronic acid grafted chitosan as a glucose-sensitive vehicle for controlled insulin release. *J. Pharm. Sci.* **2011**, *100*, 2278–86.
64. Fernández-Urrusuno, R.; Calvo, P.; Remuñán-López, C.; Vila-Jato, J.; Alonso, M. Enhancement of nasal absorption of insulin using chitosan nanoparticles. *Pharmaceut. Res.* **1999**, *16*, 1576–1581.
65. Fan, Y.; Wang, Y.; Ma, J. Preparation of insulin nanoparticles and their encapsulation with biodegradable polyelectrolytes via the layer-by-layer adsorption. *Int. J. Pharm.* **2006**, *324*, 158–67.
66. Mao, S.; Bakowsky, U.; Jintapattanakit, A.; Kissel, T. Self-assembled polyelectrolyte nanocomplexes between chitosan derivatives and insulin. *J. Pharm. Sci.* **2006**, *95*, 1035–48.
67. Calvo, P.; Remunan-Lopez, C.; Vila-Jato, J.; Alonso, M. Novel Hydrophilic Chitosan–Polyethylene Oxide Nanoparticles as Protein Carriers. *J. Appl. Polym. Sci.* **1997**, *63*, 125-132.
68. Mattu, C.; Li, R.; Ciardelli, G. Chitosan nanoparticles as therapeutic protein nanocarriers: the effect of pH on particle formation and encapsulation efficiency. *Polym. Compos.* **2013**, *34*, 1538–1545.
69. Jeffrey, D.; Anil, K. Characterization of nanoparticles intended for drug delivery: Zeta Potential Measurement. Mumbai, India: Humana Press, **2011**.

70. Zhang, X.; Zhang, H.; Wu, Z.; Wang, Z.; Niu, H.; Li, C. Nasal absorption enhancement of insulin using PEG-grafted chitosan nanoparticles. *Eur. J. Pharm. Biopharm.* **2008**, *68*, 526–34.
71. Zhu, S.; Qian, F.; Zhang, Y.; Tang, C.; Yin, C. Synthesis and characterization of PEG modified N-trimethylaminoethylmethacrylate chitosan nanoparticles. *Eur. Polym. J.* **2007**, *43*, 2244–2253.